

The immune repressor BIR1 contributes to antiviral defense and undergoes transcriptional and post-transcriptional regulation during viral infections

Irene Guzmán-Benito^{1,2} , Livia Donaire¹ , Vítor Amorim-Silva³ , José G. Vallarino³ , Alicia Esteban³ , Andrzej T. Wierzbicki⁴ , Virginia Ruiz-Ferrer¹  and César Llave¹ 

¹Departamento de Biotecnología Microbiana y de Plantas, Centro de Investigaciones Biológicas, CSIC, 28040 Madrid, Spain; ²Doctorado en Biotecnología y Recursos Genéticos de Plantas y Microorganismos Asociados, ETSI Agronómica, Alimentaria y de Biosistemas, Universidad Politécnica de Madrid, 28040 Madrid, Spain; ³Departamento de Biología Molecular y Bioquímica, Instituto de Hortofruticultura Subtropical y Mediterránea 'La Mayora', Universidad de Málaga-CSIC (IHSM-UMA-CSIC), Universidad de Málaga, Campus Teatinos, 29071 Málaga, Spain;

⁴Department of Molecular, Cellular, and Developmental Biology, University of Michigan, Ann Arbor, MI 48109, USA

Summary

Author for correspondence:
César Llave

Tel: +34 91 8373112

Email: cesarllave@cib.csic.es

Received: 2 April 2019

Accepted: 15 May 2019

New Phytologist (2019) 224: 421–438

doi: 10.1111/nph.15931

Key words: antiviral defense, BAK1, BIR1, plant innate immunity, plant viruses, post-transcriptional silencing, RNA-directed DNA methylation, SOBIR1.

- BIR1 is a receptor-like kinase that functions as a negative regulator of basal immunity and cell death in *Arabidopsis*.
- Using *Arabidopsis thaliana* and *Tobacco rattle virus* (TRV), we investigate the antiviral role of BIR1, the molecular mechanisms of *BIR1* gene expression regulation during viral infections, and the effects of BIR1 overexpression on plant immunity and development.
- We found that SA acts as a signal molecule for *BIR1* activation during infection. Inactivating mutations of *BIR1* in the *bir1-1* mutant cause strong antiviral resistance independently of constitutive cell death or SA defense priming. *BIR1* overexpression leads to severe developmental defects, cell death and premature death, which correlate with the constitutive activation of plant immune responses.
- Our findings suggest that BIR1 acts as a negative regulator of antiviral defense in plants, and indicate that RNA silencing contributes, alone or in conjunction with other regulatory mechanisms, to define a threshold expression for proper BIR1 function beyond which an autoimmune response may occur. This work provides novel mechanistic insights into the regulation of *BIR1* homeostasis that may be common for other plant immune components.

Introduction

To defend themselves against invaders, plants have evolved potent inducible immune responses (Dangl & Jones, 2001). The frontline of active defense relies on the recognition of conserved microbial components named pathogen-associated molecular patterns (PAMPs) by membrane-localized receptor-like kinases (RLKs) and receptor-like proteins (RLPs) to induce PAMP-triggered immunity (PTI) (Boller & Felix, 2009; Tena *et al.*, 2011). PTI prevents colonization by pathogens such as bacteria, fungi and oomycetes and includes activation of mitogen-activated protein kinases (MAPKs), production of reactive oxygen species (ROS), generation of the signal molecule salicylic acid (SA), differential expression of genes, callose deposition and stomatal closure (Dodds & Rathjen, 2010). Pathogens hit back by producing effectors that suppress different steps of PTI, resulting in effector-triggered susceptibility (ETS) (Jones & Dangl, 2006). As a counter-counter defense strategy, plants possess a repertoire of polymorphic disease resistance (R) proteins containing nucleotide-binding (NB) and leucine-rich repeat (LRR) domains (Martin *et al.*, 2003; Meyers *et al.*, 2003). These R immune receptors can

sense effectors directly or indirectly and establish Effector-Triggered-Immunity (ETI). ETI responses significantly overlap with PTI signaling cascades, albeit with a stronger amplitude, and often result in a form of programmed cell death at the infection sites that restricts pathogen progression (Coll *et al.*, 2011).

Recent studies show that RNA silencing is a key regulatory checkpoint modulating both PTI and ETI responses in plants (Zvereva & Pooggin, 2012; Boccara *et al.*, 2014). There is growing evidence of the role of PAMP-responsive microRNAs (miRNAs) and small interfering RNAs (siRNAs) in plant innate immunity against microbial pathogens (Katiyar-Agarwal *et al.*, 2006, 2007; Navarro *et al.*, 2006, 2008; Li *et al.*, 2010, 2014; Zhang *et al.*, 2011; Campo *et al.*, 2013; Boccara *et al.*, 2014; Ouyang *et al.*, 2014), and it is well documented how small RNA (sRNA) regulatory networks exert extensive post-transcriptional control of disease resistance genes to prevent undesirable R-mediated autoimmunity in unchallenged plants (Yi & Richards, 2007; Zhai *et al.*, 2011; Boccara *et al.*, 2014). Furthermore, RNA-directed DNA methylation (RdDM) provides epigenetic control of plant defenses by targeting transposable elements and their adjacent defense genes (Downen *et al.*, 2012; Yu *et al.*, 2013; Lopez Sanchez *et al.*, 2016).

Immune responses against viruses are thought to rely mostly on ETI upon recognition of virus-specific effectors by intracellular immune-R receptors (Zvereva & Pooggin, 2012). In this line, interesting connections between RNA silencing-mediated regulation of R genes and viral infections have been made. For instance, Brassica miR1885 is induced specifically by *Turnip mosaic virus* (TuMV) infection, and targets NB-LRR class disease-resistant transcripts for cleavage (He *et al.*, 2008). Also, members of the miR482/2118 superfamily mediate silencing of multiple NB-LRR disease resistance genes in tomato, which includes production of RNA-dependent RNA polymerase 6 (RDR6)-dependent secondary siRNAs (Shivaprasad *et al.*, 2012). Interestingly, the miR482-mediated silencing cascade is suppressed in plants infected with viruses or bacteria allowing pathogen-inducible expression of NB-LRR targets (Shivaprasad *et al.*, 2012). In another study, two miRNAs (miR6019 and miR6020) guide cleavage and production of functional secondary siRNAs from transcripts of the NB-LRR immune receptor *N* from tobacco that confers resistance to *Tobacco mosaic virus* (TMV) (Li *et al.*, 2012). Overexpression of both miRNAs attenuates *N*-mediated resistance to TMV, demonstrating that miRNAs and secondary siRNAs have a functional role in regulating resistance to TMV.

Although in plants, there are apparently no equivalent PAMPs derived from viruses, several studies have suggested a role of PTI in antiviral defense (Korner *et al.*, 2013; Gouveia *et al.*, 2016; Nicaise & Candresse, 2017). For instance, a recent report shows that Arabidopsis mutants deficient in the PTI master regulator *BRASSINOSTEROID INSENSITIVE1 (BRI1)-ASSOCIATED RECEPTOR KINASE1 (BAK1)* exhibit increased susceptibility to different RNA viruses (Korner *et al.*, 2013). BAK1 interacts *in vivo* with the RLK BAK1-INTERACTING RECEPTOR-LIKE KINASE 1 (BIR1), a negative regulator of PTI responses and cell death pathways in Arabidopsis (Gao *et al.*, 2009). It has been suggested that BIR1 sequesters BAK1 to prevent unwanted interactions with ligand-binding receptors in the absence of pathogens (Gao *et al.*, 2009; Ma *et al.*, 2017). Here, we study the role of BIR1 during viral infections and the molecular mechanisms whereby *BIR1* is regulated. We further show that *BIR1* regulation is critical to avoid constitutive activation of plant defense responses, which drastically impairs plant fitness and growth.

Materials and Methods

Plant material

Nicotiana benthamiana and *Arabidopsis thaliana* plants were grown in controlled environmental chambers under long-day conditions (16 h : 8 h, light : dark) at 25°C and 22°C, respectively. Arabidopsis lines used in this study were derived from the Columbia-0 (Col-0) ecotype. Mutants for *bir1-1* and *sobir1-12* and *bir1-1/BIR1* lines were donated by Yuelin Zhang (University of British Columbia, Canada). The Arabidopsis *ago1-27*, *ago1-25*, *ago2-1* and mutant combinations involving the alleles *rdrl-1*, *rdrl-2*, *rdrl-15*, *dcl2-1*, *dcl3-1* and *dcl4-2* were donated by James C. Carrington (The Donald Danforth Plant Center, Creve Coeur, MO, USA). Arabidopsis mutant *cmt3* and *ddc* were supplied by Steve

Jacobsen (UCLA-HHMI, Los Angeles, CA, USA). The Arabidopsis *nrpe1 (nrpd1b-1)* was donated by Craig Pikaard (Indiana University, IN, USA). The Arabidopsis mutant *drm2-2* was supplied by Eric Richards (Boyce Thompson Institute, Cornell University, NY, USA). The Arabidopsis *npr1-1* and NPR1ox seeds were supplied by Xinning Dong (Duke University, NC, USA).

Construction of a recombinant TRV-BIR1 vector and viral inoculation

Tobacco rattle virus (TRV) derivatives were created from an infectious TRV clone (Liu *et al.*, 2002). TRV-GFP contained the HA-tagged soluble modified green fluorescence protein (GFP) under the promoter region of the *Pea early browning virus* (PEBV) replicase (Fernandez-Calvino *et al.*, 2016a). TRV-BIR1 contained the Arabidopsis *BIR1* coding region under the PEBV promoter. Briefly, the *BIR1* cDNA containing its 5' UTR was amplified by reverse transcription polymerase chain reaction (RT-PCR), cloned into the Gateway pDONR207 vector, and shuffled into the binary destination vector pGWB14. The human influenza hemagglutinin (HA)-tagged BIR1 sequence was then PCR-amplified, and cloned into pTRV2. The recombinant clones were screened by restriction enzyme digestion and sequencing. TuMV-GFP was derived from an infectious clone of the TuMV strain UK1 (Lellis *et al.*, 2002). All primers used in this study are listed in Supporting Information Table S1.

Nicotiana benthamiana plants were inoculated at *c.* 21 d after germination by infiltration of agrocultures containing TRV or TuMV (Johansen & Carrington, 2001; Liu *et al.*, 2002). Three-week-old Arabidopsis plants were inoculated using sap extracts from virus-infected *N. benthamiana* leaves as previously described (Fernandez-Calvino *et al.*, 2014). Arabidopsis plants inoculated with sap from noninfiltrated *N. benthamiana* were used as controls (mock). Additionally, experiments were paralleled using naïve Arabidopsis plants to discard potential side-effects as a result of wounding caused by abrasion used during mechanical inoculation of sap extracts.

Construction of BIR1 transgenic plants

Arabidopsis Col-0 transgenic plants expressing the GFP:GUS dual reporter gene under the *BIR1* promoter were generated using the Gateway-compatible pBGWFS7 binary vector. A genomic DNA fragment of 3297 bp containing the *BIR1* promoter was cloned upstream to the fusion reporter gene as previously described (Xiao *et al.*, 2010). Arabidopsis Col-0 transgenic plants expressing *BIR1* were obtained using a glucocorticoid (dexamethasone (DEX))-inducible gene expression system (Marques-Bueno *et al.*, 2016). Briefly, the GVG::ter::6xUAS/pDONR221 contained the GVG cassette cloned into pDONR221. mCherry was added to this vector to generate GVG::ter::6xUAS::mCherry/pDONR221. pDONR221-BIR1 contained the full-length *BIR1* protein coding gene as described earlier. Final destination vectors were obtained by three-fragment recombination using the pH7m34GW destination vector. All the constructs were transformed into wild-type Col-0 plants according to standard floral

dipping (Clough & Bent, 1998). Independent homozygous lines harboring a single transgene insertion were selected in T4 and used for subsequent experiments.

Methylation analyses

Chop-qPCR was carried out as previously described (Bohmdorfer *et al.*, 2014) using genomic DNA (100 ng) from 3-wk-old Arabidopsis rosette leaves and the methylation-sensitive restriction enzymes *DdeI* and *NlaIII*. Chop quantitative PCR (Chop-qPCR) was done using Maxima Hot Start Taq DNA Polymerase (Thermo Scientific, Waltham, MA, USA) and 25× SYBR Green (Invitrogen) diluted at 1 : 400.

Bisulfite sequencing was done as previously described (He *et al.*, 2009). Briefly, genomic DNA from 3-wk-old rosette leaves was extracted using DNeasy Plant Mini Kit (Qiagen). Bisulfite conversion was done using the EZ DNA Methylation Startup kit (Zymo Research, Irvine, CA, USA). PCR was done using Maxima Hot Start Taq DNA Polymerase (Thermo Scientific), and amplification products were cloned into TOPO TA plasmids (Invitrogen). At least 30 clones per sample were sequenced. A nonmethylated region at coordinates 19 573 407–19 573 671 in chromosome 4 was included as bisulfite conversion control. Primers for bisulfite were designed as previously described (Paterson *et al.*, 2011) and listed in Table S1.

RNA analysis

Total RNA was extracted with TRIzol reagent (Invitrogen). One-step quantitative RT-PCR (qRT-PCR) was carried out using Brilliant III Ultra-Fast SYBR Green QRT-PCR Master Mix (Agilent Technologies, Cedar Creek, TX, USA) in a Rotor-Gene 6000/Rotor-Gene Q real-time PCR machine (Corbett/Qiagen, Sydney, Australia) (Fernandez-Calvino *et al.*, 2016a). Relative gene expression was determined using the Delta-delta cycle threshold method and Rotor-Gene 6000 Series Software (Corbett). Constitutively expressed *CBP20* (*At5g44200*) or *Actin2* (*At3g18780*) transcripts were used for normalization because of its similar level of expression in mock-inoculated and virus-infected leaves. A standard curve of known concentration of *in vitro* synthesized TRV transcripts was used to determine the TRV concentration as the number of viral copies per nanogram of total RNA (Fernandez-Calvino *et al.*, 2016a). Significant differences between two or among several samples were compared by Student's *t*-test or one-way ANOVA followed by Duncan's test, respectively, using STATGRAPHICS PLUS v.5.1 (Statistical Graphics Corp., The Plains, VA, USA). Unless otherwise indicated, each Arabidopsis sample used for qRT-PCR analysis consisted of RNA extracted from a pool of rosette leaves from five plants (three leaves per plant, all leaves at identical positions).

Protein analysis

Protein extracts were prepared and analyzed by immunoblot assay after sodium dodecyl sulfate-polyacrylamide gel electrophoresis (Fernandez-Calvino *et al.*, 2016b). Blotted proteins

were detected using commercial horseradish peroxidase-conjugated secondary antibodies and a chemiluminescent substrate (LiteAblo Plus, Pero, Milano, Italy). Relative protein accumulation was measured by densitometry of protein blots exposed to autoradiographic films using the IMAGEJ software.

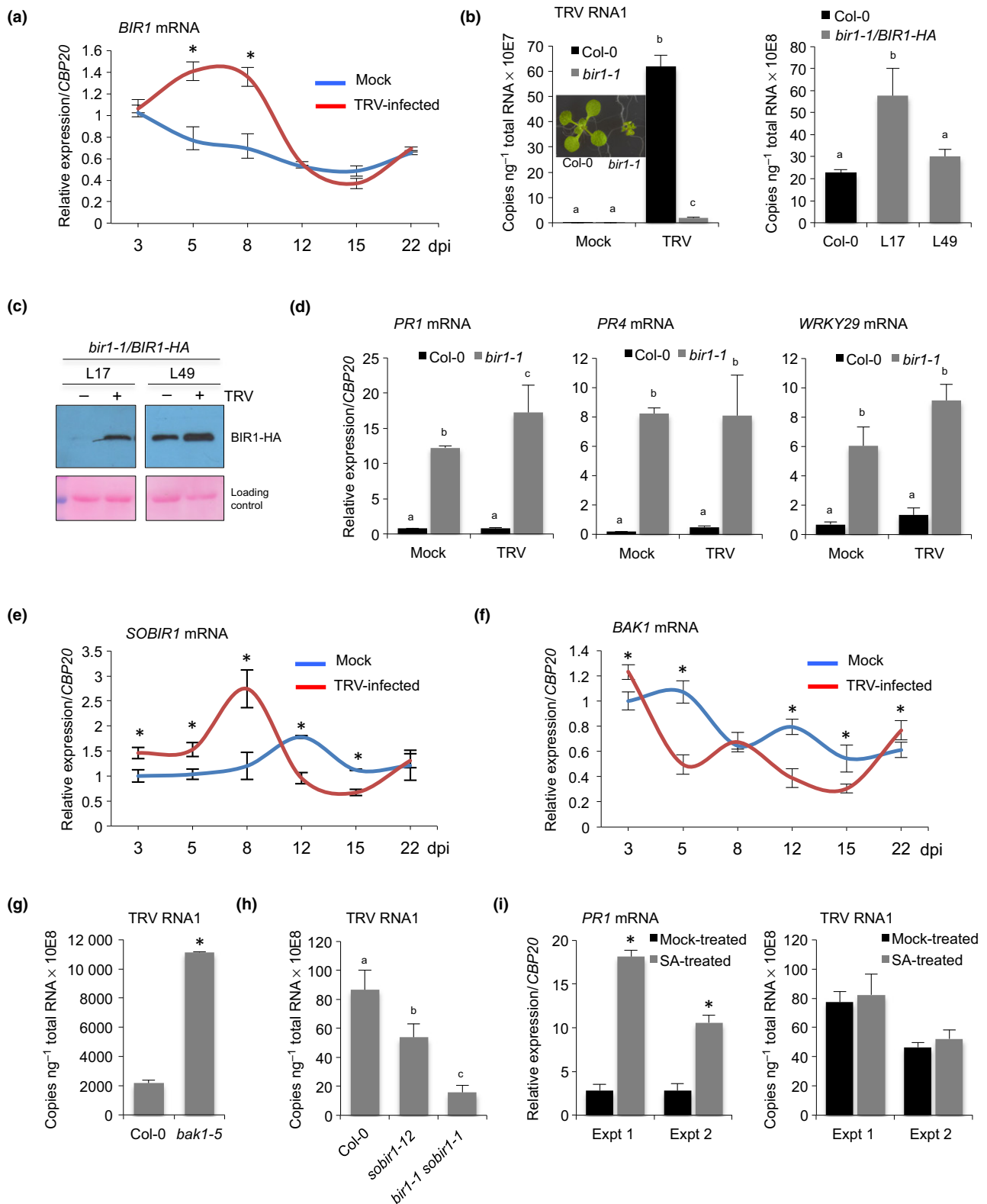
Small RNA sequencing, construction of degradome libraries and 5'-rapid amplification of cDNA ends (5'-RACE)

Young rosette leaves from virus-infected plants and the corresponding mock-inoculated plants were pooled (10–12 plants) at 8 d postinoculation (dpi) (TRV) or 14 dpi (TuMV), and used for degradome or sRNA sequencing. Systemically infected inflorescences from TRV-infected or mock-inoculated Arabidopsis were pooled (10–15 plants) at 16 dpi, and used for degradome sequencing. Total RNA was extracted using TRIzol reagent (Invitrogen) or Plant RNeasy Kit (Qiagen) and tested through the Agilent 2100 bioanalyzer system to guarantee RNA quality. sRNA libraries were prepared and sequenced on an Illumina Genome Analyzer (HiSeq2000, 1 × 50 bp, single-end run) by Ascidea Computational Biology Solutions (Barcelona, Spain, www.ascidea.com).

Parallel analysis of RNA ends degradome libraries were done as previously described (German *et al.*, 2009) and sequenced on an Illumina Genome Analyzer (HiSeq2000, 1 × 50 bp, single-end run) by Fasteris (Geneva, Switzerland; www.fasteris.com) and IGA Technology Services (Udine, Italy, www.igatechnology.com). Sequencing data were then analyzed using CLEAVELAND4 (Addo-Quaye *et al.*, 2009). Briefly, all degradome sequence reads with exact matches to structural RNA were removed and the filtered dataset was mapped against the Arabidopsis cDNA sequence transcriptome (TAIR10) using BOWTIE. For each exact match, 13-nt-long sequences upstream and downstream of the location of the 5'-end of the matching degradome sequence were extracted to create a 26-nt-long 'query' mRNA subsequence. Query sequences were then aligned to each sRNA sequence in our sRNA datasets or to miRNA reported in miRBase using GSTAR (CLEAVELAND4 pipeline) (Addo-Quaye *et al.*, 2009). A modified 5'-RACE was used for mapping internal cleavage sites as previously described (Donaire *et al.*, 2011).

SA application and determination of SA content

Three-week-old plants grown on soil were sprayed with SA (1 mM) as previously described (Takahashi *et al.*, 2007). To test the effect of SA on TRV accumulation, plants were TRV- or mock-inoculated 24 h after the first SA application and then treated for 8 d consecutively by spraying the solution once at intervals of 24 h (Expt 1) or 48 h (Expt 2). To assess SA content in the plant tissue, rosette leaves were harvested at the same leaf position in order to minimize variations in the hormone content throughout the plant. SA was extracted and derivatized as previously described (Vallarino & Osorio, 2016). The samples were analyzed using GC coupled to time-of-flight MS (GC-TOF-MS) (Pegasus III, Leco, Mönchengladbach, Germany), and quantified using an internal standard ($[^2\text{H}_4]$ -SA; OlChemIm Ltd, Olomouc, Czech Republic).



Accession numbers

DNA methylation data (GSE39901) were used from Stroud *et al.* (2013). Degradome sequencing data from naïve Col-0

inflorescences (GSM280226) were reported previously (German *et al.*, 2008). Sequence data from this article can be found in the NCBI Gene Expression Omnibus (GEO; <http://www.ncbi.nlm.nih.gov/geo/>) under accession nos. GSM3019138,

Fig. 1 Expression of *BIR1*, *SOBIR1* and *BAK1* during *Tobacco rattle virus* (TRV) infection in Arabidopsis and effect of their loss-of-function mutations on TRV accumulation. (a) Time-course accumulation of *BIR1* transcripts in mock-inoculated and TRV-infected leaves. (b) Accumulation of TRV genomic RNA in TRV-infected rosette leaves of Arabidopsis wild-type (Col-0), *bir1-1* mutants (left) and two *bir1-1/BIR1-HA* complemented lines (L17 and L49) (right) at 8 d postinoculation (dpi). Mock-inoculated controls were included in the left panel to discriminate background amplification. The phenotype of wild-type and *bir1-1* plants grown on MS medium at 21°C is shown. (c) Western blot analysis of BIR1 proteins in extracts from leaves of mock-inoculated (–) or TRV-infected (+) *bir1-1/BIR1-HA* complemented lines (L17 and L49) at 8 dpi. Ponceau staining was used as a protein loading control. (d) Accumulation of defense-related *PR1*, *PR4*, and *WRKY29* transcripts in mock-inoculated or TRV-infected leaves of Arabidopsis wild-type and *bir1-1* mutants at 8 dpi. (e) Time-course accumulation of *SOBIR1* transcripts in mock-inoculated and TRV-infected leaves. (f) Time-course accumulation of *BAK1* transcripts in TRV-infected and mock-inoculated leaves. (g) Accumulation of TRV genomic RNA in rosette leaves of wild-type and *bak1-5* mutants at 8 dpi. (h) Accumulation of TRV genomic RNA in rosette leaves of wild-type, *sobir1-12* and *sobir1 bir1* mutants at 8 dpi. (i) Accumulation of *PR1* transcripts (left) and TRV genomic RNA (right) in rosette leaves of wild-type plants treated with or without (mock) salicylic acid (SA). Expts 1 and 2 are described in the Materials and Methods section. Relative expression levels were determined by quantitative reverse transcription polymerase chain reaction (qRT-PCR) and normalized to the *CBP20* internal control. Error bars represent SD from three independent PCR measurements. Values in (a), (e) and (f) are related to the mock-inoculated sample at 3 dpi that was arbitrarily assigned to 1. Asterisks (Student's *t*-test) or different letters (one-way ANOVA) were used to indicate significant differences ($P < 0.001$). The experiments were repeated at least three times with similar results and one representative biological replicate is shown.

GSM3019139, GSM3019140 (deep sequencing of degradome tags), and GSM2808011, GSM2808012, GSM3019141, GSM3019142 (deep sequencing of sRNAs).

Results

Inactivating mutations in the immune repressor BIR1 triggers resistance to TRV

To gain an insight into the role of Arabidopsis *BIR1* (*At5g48380*) in the infectious process, we monitored *BIR1* expression during infection with TRV in a time-course experiment. We found that *BIR1* transcripts were significantly induced in leaves of TRV-infected plants at 5 and 8 dpi compared with mock-inoculated controls (Fig. 1a). *BIR1* was also upregulated in response to the unrelated TuMV (Fig. S1a). Using an Arabidopsis *bir1-1* mutant, we found that depletion of *BIR1* led to strong antiviral resistance against TRV (Fig. 1b). However, TRV levels reverted back to those of wild-type plants, or even higher, in *bir1-1*-complemented lines (*bir1-1/BIR1-HA*) expressing an HA-tagged wild-type BIR1 coding gene (Fig. 1b). This result confirmed that the resistance phenotype observed in *bir1-1* was caused by mutation in *BIR1*. Western blot assay using anti-HA antibody also revealed a significant induction of BIR1 protein in *bir1-1/BIR1-HA* lines after TRV infection, indicating that elevated *BIR1* transcript abundance reflected protein abundance in systemically infected leaves (Fig. 1c). The *bir1-1* mutant is known to constitutively activate cell death and defense responses that are partially dependent on the SA-dependent resistance pathway (Gao *et al.*, 2009; Liu *et al.*, 2016). Accordingly, we found that transcription of the defense marker genes *PR1*, *PR4*, *PAD3* and *WRKY29* remained similarly reactivated in TRV-infected *bir1-1* mutants, indicating that virus infection does not impair the activation of defense when *BIR1* is genetically suppressed (Figs 1d, S1b). The autoimmune phenotypes in *bir1-1* mutants are partially dependent on *SUPPRESSOR OF BIR1-1 1* (*SOBIR1*), which promotes cell death and defense in conjunction with BAK1 (Chinchilla *et al.*, 2007; Gao *et al.*, 2009; Liu *et al.*, 2016). Interestingly, we found a significant induction of *SOBIR1* transcripts in Arabidopsis leaves at early time points of TRV or TuMV infection compared with mock-inoculated plants (Figs 1e, S1a,c). By contrast,

BAK1 transcripts decreased significantly after infection with TRV or TuMV (Figs 1f, S1a,c). In our assay, the *bak1-5* mutant, which is strongly impaired in PTI signaling (Schwessinger *et al.*, 2011), was more susceptible to TRV accumulation (Fig. 1g), whereas TRV levels were moderately diminished in *sobir1-12* mutants (Fig. 1h). Importantly, TRV RNA levels were also drastically reduced in a *sobir1-1 bir1-1* double mutant, in which cell death and SA-dependent defense responses are significantly reduced by the *sobir1-1* mutation (Gao *et al.*, 2009). This result suggested that TRV resistance associated with loss of *BIR1* function in the *bir1-1* mutant was unrelated to constitutive cell death or SA defense priming (Fig. 1i). Consistent with this notion, we showed that exogenous application of SA triggered accumulation of *PR1* transcripts in the plant tissue but was not sufficient to prime plant defense against TRV (Fig. 1i). Collectively, our results indicated that TRV triggers an immune response in which BIR1 probably functions as a negative regulator of antiviral defenses.

RdDM imparts transcriptional control of *BIR1*

Inspection of Arabidopsis sRNA sequencing datasets generated in our laboratory revealed the profuse accumulation of siRNAs upstream of the *BIR1* transcription start site, the vast majority of which corresponded to the 24 nt class (Figs 2a, S1d). As 24 nt siRNAs guide methylation in the canonical RdDM pathway (Xie & Yu, 2015), we investigated if siRNA-dependent RdDM controls *BIR1* expression. First, *BIR1* transcripts were significantly more abundant in the RdDM mutants *drm2*, *drm1 drm2 cmt3* (herein *ddc*), *nrpe1* and *ago4* mutants compared with wild-type plants (Fig. 2b). *BIR1* levels were unaffected in the single *cmt3* mutant, probably as a result of redundancy between methyltransferases DRM2 and CMT3 in maintaining nonCG DNA methylation (Fig. 2b) (Cao & Jacobsen, 2002). We then used qRT-PCR to detect RNA products at the intergenic region containing the predicted *BIR1* promoter. Interestingly, transcripts were amplified in wild-type Col-0 plants but not in *nrpe1* mutants, indicating that Pol V was required for their production (Fig. 2c). The accumulation of Pol V-dependent transcripts derived from *INTERGENIC LOCUS 22* (*IGN22*) was used as a positive control (Rowley *et al.*, 2011) (Fig. S2a).

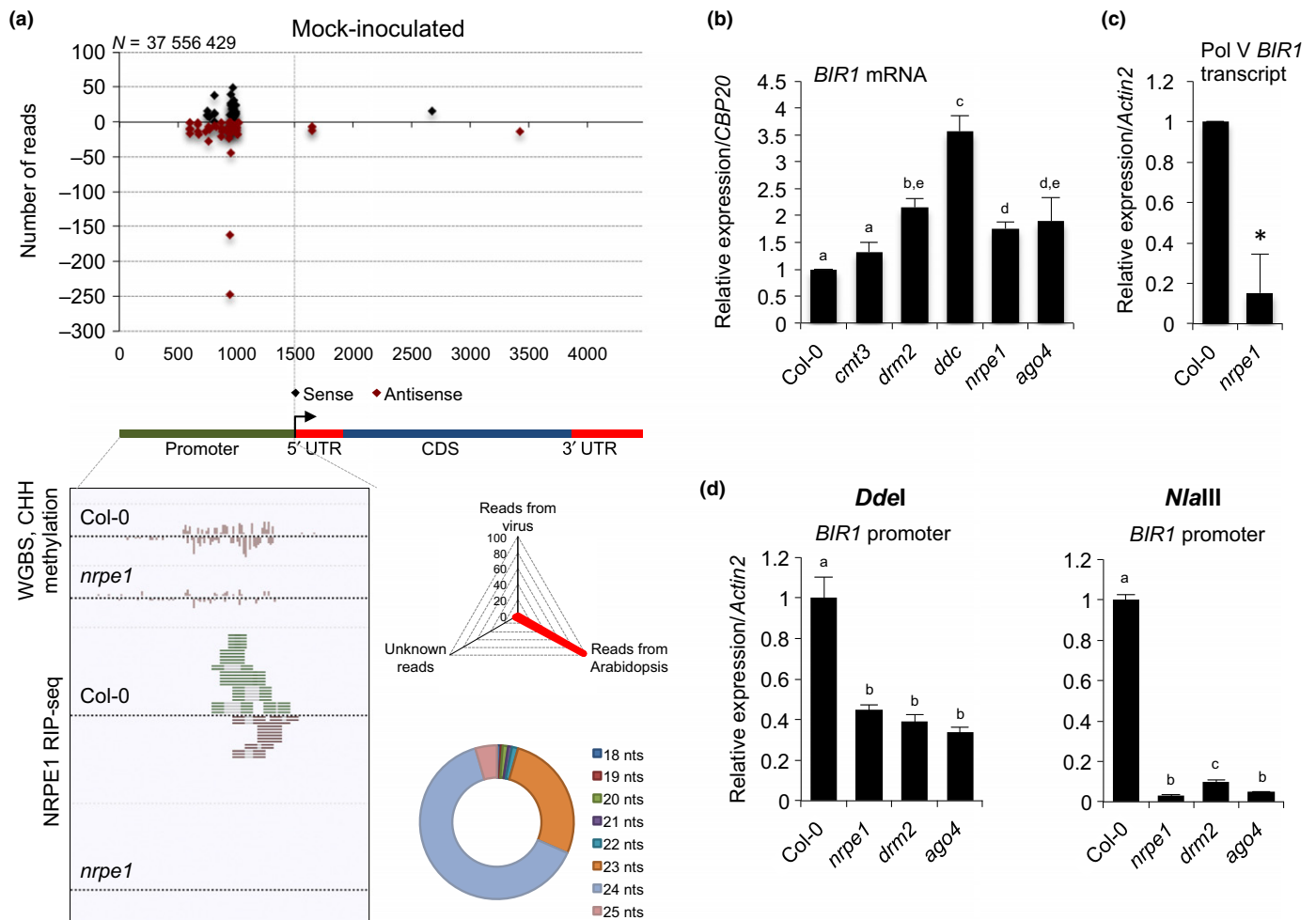


Fig. 2 RNA-directed DNA methylation (RdDM)-mediated transcriptional regulation of *BIR1*. (a) Distribution of *BIR1*-derived small interfering RNAs (siRNAs) in rosette leaves of mock-inoculated Arabidopsis plants (upper diagram). Sense (black dots) and antisense (red dots) siRNA species are represented as positive and negative values on the y-axis, respectively. The triangle graph represents the genomic distribution (percentage) of siRNAs in the sequenced set. N denotes the total number of filtered sequenced reads. The circle graph represents the size distribution of *BIR1*-derived siRNAs. The genome browser screenshot of CHH methylation and Pol V transcripts at the *BIR1* promoter in wild-type (Col-0) and *nrpe1* mutants using whole-genome bisulfite sequencing (WGBS) and Pol V (NRPE1) RIP-seq datasets is shown (Wierzbicki *et al.*, 2012; Bohmdorfer *et al.*, 2016) (lower diagram). (b) Accumulation of *BIR1* transcripts in rosette leaves of wild-type and RdDM mutants (*cmt3*, *drm2*, *ddc*, *nrpe1* and *ago4*). (c) Accumulation of Pol V-dependent *BIR1* promoter transcripts in rosette leaves of wild-type and *nrpe1* mutants. (d) Extent of asymmetric (CHH) cytosine methylation at the *BIR1* promoter determined by Chop-qPCR in rosette leaves of wild-type and RdDM mutants (*nrpe1*, *drm2* and *ago4*). PCR-amplified regions contain recognition sites of the methylation-sensitive *DdeI* and *NlaIII* endonucleases. Relative expression levels were determined by quantitative reverse transcription polymerase chain reaction (qRT-PCR) and normalized to the *CBP20* or *Actin2* internal control as indicated. Error bars represent SD from three independent PCR measurements. Asterisks (Student's *t*-test) or different letters (one-way ANOVA) were used to indicate significant differences ($P < 0.001$). The experiments were repeated at least three times with similar results and one representative biological replicate is shown.

If *BIR1* were an RdDM target, DNA methylation at this locus should be reduced in RdDM mutants. To test this idea, we performed methylation-specific Chop-qPCR to examine DNA methylation at the *BIR1* promoter region in wild-type and several DNA methylation mutants. Genomic DNA was digested with the CHH methylation-sensitive restriction endonucleases *DdeI* and *NlaIII* before PCR amplification using flanking primers (Bohmdorfer *et al.*, 2014). We found amplification products in DNA samples treated with either *DdeI* or *NlaIII* in the wild-type background, indicative of active cytosine methylation (Fig. S2b). By contrast, low levels of amplification were reported in the RdDM mutants *nrpe1*, *drm2* or *ago4* (Fig. S2b). Similar results

were obtained for *At1g49490* and *IGN36*, used as positive RdDM controls for *DdeI* and *NlaIII* digestions, respectively (Bohmdorfer *et al.*, 2014) (Fig. S2b). Parallel amplification of DNA sequences without restriction sites (*At1g55535* and *At2g36490*) from the same digested DNA samples, used as internal digestion controls, produced amplification bands in all genetic backgrounds (Fig. S2b). Quantification of the difference in DNA methylation by Chop-qPCR indicated that CHH methylation at both the *BIR1* promoter and the *At1g49490* and *IGN36* positive controls, but not the negative control, was reduced to a similar extent in all mutants tested (Figs 2d, S2c). Finally, whole-genome bisulfite sequencing (WGBS) reported by

Wierzbicki *et al.* (2012) revealed extensive symmetrical and asymmetrical DNA methylation in the *BIR1* promoter, whereas methylation was drastically diminished in *nrpe1* compared with wild-type plants (Figs 2a, S3). Furthermore, published Pol V RIP-seq data (Bohmdorfer *et al.*, 2016) revealed that Pol V-associated RNA accumulated in the Col-0 wild-type, but not in *nrpe1* mutants, confirming that RNA reads originated at the *BIR1* promoter were associated with Pol V (Fig. 2a). Collectively, our data demonstrated that *BIR1* was an RdDM target under normal growing conditions.

SA mediates transcriptional activation of *BIR1* during TRV infection

We wondered whether higher accumulation of *BIR1* transcripts in infected tissues could reflect the transcriptional activation of the *BIR1* locus in response to the virus. To test this idea, Arabidopsis plants expressing a GFP:GUS fusion protein under the control of the *BIR1* promoter were challenged with TRV. GUS activity was strongly and consistently induced in rosette leaves and aerial tissues of TRV-infected transgenic plants when compared with the mock-inoculated ones (Fig. 3a). The spatial pattern of GUS induction suggested that *BIR1* responded ubiquitously to TRV infection. Furthermore, Northern blot revealed higher abundance of GFP:GUS fusion transcripts in the presence of TRV, confirming that TRV triggered transcriptional activation of *BIR1* (Fig. 3a).

Inspection of transcriptomic data revealed that two key SA biosynthetic genes, *ICS1* and *PAD4* (Chen *et al.*, 2009), were significantly upregulated in leaves of TRV-infected plants (Fig. 3b) (Fernandez-Calvino *et al.*, 2014). We thus wondered if SA concentrations influence *BIR1* expression in the infected tissue. To test this possibility, we first determined the concentrations of SA in the leaves of soil-grown plants using GC-TOF-MS. SA concentrations gradually increased from 5 to 14 dpi in TRV-infected plants, whereas they remained constant in both uninoculated and mock-inoculated plants (Fig. 3c). We found that *BIR1* transcripts were markedly enhanced in wild-type Arabidopsis at 6 h after SA application compared with mock-treated controls (Fig. 3d). Furthermore, we observed increasing abundance of GFP:GUS transcripts in Arabidopsis plants expressing a GFP:GUS reporter under the *BIR1* promoter at 6, 12 and 24 h after SA treatment, indicating that SA efficiently promotes transcriptional activation of *BIR1* (Fig. 3e). Importantly, SA activation of *BIR1* during TRV infection was largely inhibited in the Arabidopsis *sid2-2* mutant, which has disrupted the pathogen-inducible *ICS1* gene and reduced SA accumulation (Wildermuth *et al.*, 2001) (Fig. 3f). We also found that induction of *BIR1* in virus-infected plants was compromised in *npr1-1* Arabidopsis mutants, which lack NPR1 receptor-dependent SA signaling (Cao *et al.*, 1997; Wu *et al.*, 2012), compared with wild-type or *npr1*-complemented transgenic lines (OxNPR1) (Fig. 3g). These findings indicated that SA acts as a signal molecule for *BIR1* activation during TRV infection, and that TRV promotes *BIR1* expression by increasing the concentrations of SA in infected cells. Interestingly, TRV levels in the SA-deficient *sid2-2* mutants were lower

than those in wild-type plants, whereas plants with the *npr1-1* mutation display enhanced susceptibility to TRV (Fig. 3h). Our results support the idea that SA lacks direct antiviral functions against TRV and suggest an SA-independent role for NPR1 in the control of TRV infection.

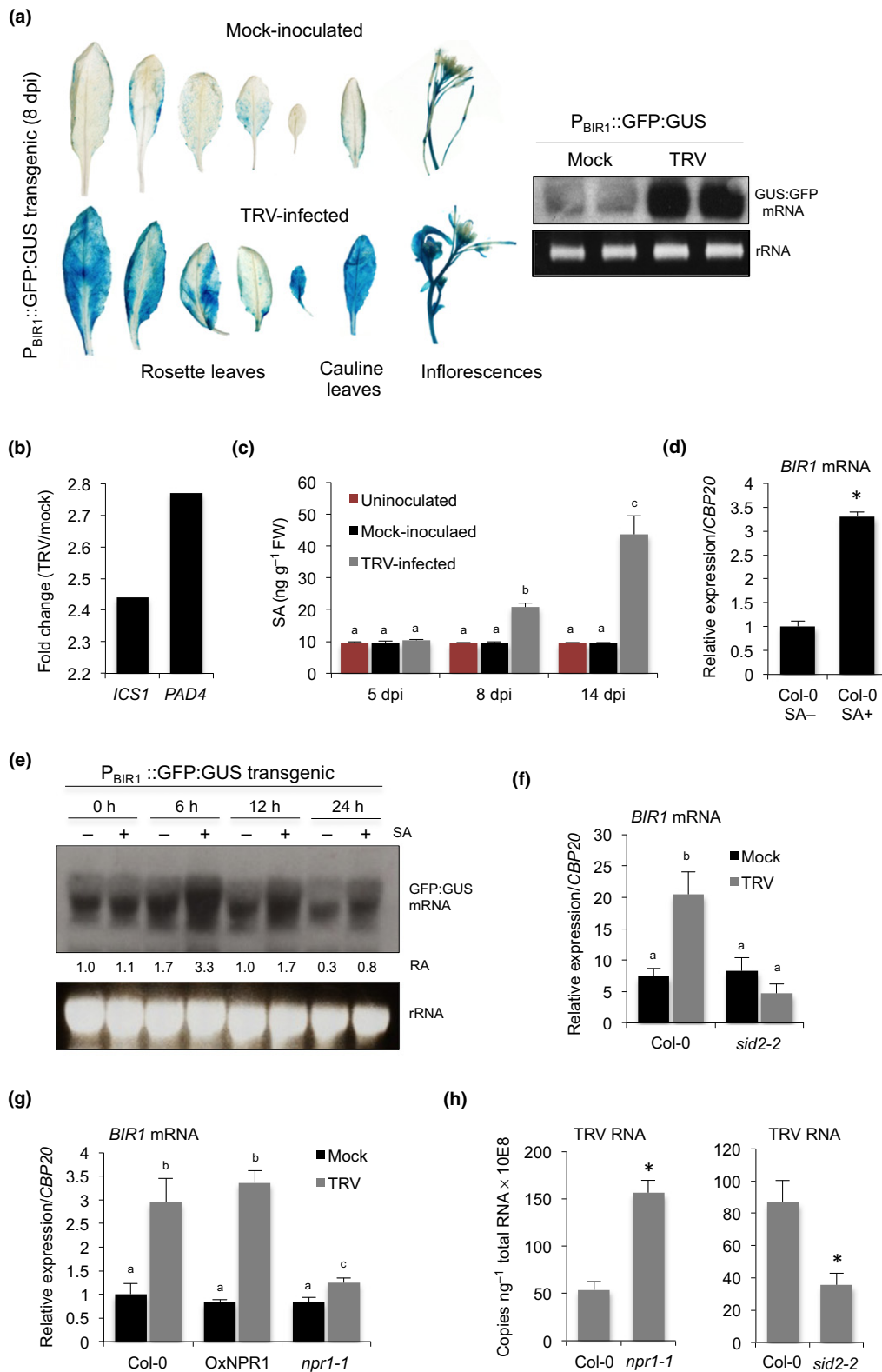
TRV activates *BIR1* without affecting its methylation status

We next asked if *BIR1* induction in infected plants was a result of changes in the methylation status of its promoter. We found that siRNAs of 24 nts produced upstream of the *BIR1* transcription start were as abundant in TRV-infected plants as in mock-inoculated controls, suggesting that epigenetic silencing of *BIR1* was not compromised by TRV (Fig. 4a). Chop-qPCR experiments revealed comparable levels of CHH methylation at the *BIR1* promoter in mock-inoculated and TRV-infected samples after digestion with *NlaIII*, whereas the relative levels of amplified DNA were slightly reduced in infected samples digested with *DdeI*, possibly as a result of star activity of the enzyme (Fig. 4b). No significant changes in the CHH methylation of the RdDM targets *At1g49490* and *IGN36*, used as methylation controls, were observed in plants exposed to TRV infection relative to the mock-inoculated ones (Fig. S2d). *BIR1* was induced by TRV to a similar extent in all RdDM mutants (except *drm2*), suggesting that TRV supported *BIR1* transcription regardless of its methylation status (Fig. 4c). Importantly, *BIR1* transcripts were elevated in TRV-infected *ddc*, *nrpe1* or *ago4* mutants compared with wild-type plants, indicating that RdDM was important to contain *BIR1* expression during infection (Fig. 4c). Finally, similar patterns of methylation at the *BIR1* promoter were observed in healthy, mock-inoculated and virus-infected plants when methylation was analyzed using locus-specific bisulfite sequencing (Figs 4d, S4).

We next investigated whether SA altered the DNA methylation pattern of the *BIR1* promoter. We found low levels of DNA amplification diagnostic of loss of asymmetric methylation in *nrpe1*, *drm2* or *ago4* mutants compared with wild-type Col-0 plants after 6 or 12 h of SA treatment (Fig. S5a,b). DNA methylation at the *At1g49490* and *IGN36* controls diminished in RdDM mutants regardless of SA treatments (Fig. S5a). *BIR1* transcripts increased after SA treatment in wild-type plants and in *nrpe1*, *drm2* or *ago4* mutants, indicating that loss of DNA methylation did not compromise SA-mediated induction of *BIR1* (Fig. S5c). Finally, transcription at the *BIR1* promoter was strongly reduced in the Pol V-defective *nrpe1* mutants in leaves of both mock-treated and SA-sprayed plants (Fig. S5d). Collectively, our data proved that SA activates transcription of *BIR1* during virus infections without interfering with its epigenetic regulation.

BIR1 is regulated by post-transcriptional RNA silencing

The analysis of our sRNA sequences revealed that siRNAs matching the *BIR1* protein-coding region were abundant in plants systemically infected with TRV or TuMV, but not in mock-inoculated ones, suggesting that *BIR1* is a target of post-transcriptional silencing during infections (Figs 2a, 4a,e, S1d,f). To test this possibility, we first monitored *BIR1* transcripts in



noninfected *Arabidopsis* silencing mutants. Although data between independent repeats showed slight variations, a subtle increment of *BIR1* transcripts in some mutants involving dysfunctional *DCL2*, *DCL3* or *DCL4* as well as in mutants with genetic defects in *RDR1*, *RDR2* or *RDR6* suggested that *BIR1*

may undergo conditional post-transcriptional silencing under nonchallenging conditions (Figs 5a, S6a).

When *BIR1* transcripts were measured in TRV-infected plants, we found that *BIR1* was induced in the double *dcl2 dcl3* mutants as much as the wild-type (Fig. 5a). By contrast, *BIR1* transcripts were

Fig. 3 Salicylic acid (SA)-mediated transcriptional activation of *BIR1* during viral infection. (a) Histochemical localization of β -glucuronidase (GUS) expression in mock-inoculated and *Tobacco rattle virus* (TRV)-infected transgenic *Arabidopsis* plants expressing a GFP:GUS fusion protein under the control of the *BIR1* promoter (left panel). Northern blot analysis was used to monitor the expression of GFP:GUS mRNA using a green fluorescent protein (GFP)-specific radiolabeled probe (right panel). Ethidium bromide-stained RNA (before transfer) is shown as loading control. (b) Differential expression of SA biosynthetic genes *ICS1* and *PAD4*. Fold-change (\log_2) in TRV-infected plants relative to mock-inoculated ones detected using a complete *Arabidopsis* transcript microarray (CATMA) (GSE15557) (Fernandez-Calvino *et al.*, 2014). (c) Time-course accumulation of SA determined by GC-time-of-flight-MS in leaves of uninoculated, mock-inoculated and TRV-infected *Arabidopsis*. Error bars represent SD from five independent biological replicates. (d) Accumulation of *BIR1* transcripts in rosette leaves of wild-type (Col-0) plants treated with (+) or without (–) SA as indicated. (e) Northern blot analysis of GFP:GUS mRNA in extracts from transgenic leaves treated with (+) or without (–) SA as indicated. Samples were collected at 0, 6, 12 and 24 h post-treatment and blots were hybridized with a GFP-specific DNA-radiolabeled probe. Ethidium bromide-stained RNA (before transfer) is shown as loading control. The relative accumulation (RA) level for each sample is indicated (in mock-treated plants at 0 h this was arbitrarily set at 1.0). (f) Accumulation of *BIR1* transcripts in mock-inoculated and TRV-infected rosette leaves of wild-type and *sid2-2* mutants at 8 d postinoculation (dpi). (g) Accumulation of *BIR1* transcripts in mock-inoculated and TRV-infected rosette leaves of wild-type, NPR1 overexpressor and *npr1-1* mutants at 8 dpi. (h) Accumulation of TRV genomic RNA in rosette leaves of wild-type, *npr1-1* and *sid2-2* mutants at 8 dpi. Relative expression levels were determined by quantitative reverse transcription polymerase chain reaction and normalized to the *CBP20* internal control. Unless otherwise indicated, error bars represent SD from three independent PCR measurements. Asterisks (Student's *t*-test) or different letters (one-way ANOVA) were used to indicate significant differences ($P < 0.001$). The experiments were repeated at least twice with similar results, and one representative biological replicate is shown.

significantly more abundant in *dcl2 dcl4*, *dcl3 dcl4* or *dcl2 dcl3 dcl4* mutants compared with control plants, indicating that DCL4 was important to prevent excessive *BIR1* accumulation in the infected tissue (Fig. 5a). Similarly, *BIR1* transcripts were, in general, far more abundant in *rdp2 rdp6* and, to a lower extent, in *rdp1 rdp6* and *rdp1 rdp2 rdp6* defective mutants than in wild-type infected plants (Fig. 5a). Finally, *BIR1* transcripts were similar in mock-inoculated wild-type and *ago1* mutants, whereas *BIR1* transcripts were more abundant in *ago1* when they were infected (Fig. 5a). Similar results were observed in plants systemically infected with TuMV, suggesting that post-transcriptional RNA silencing was accentuated in response to viral infections (Fig. S1e).

To support our findings, we examined *BIR1* mRNA degradation via degradome sequencing. By plotting the abundance of 5' signatures matching the *BIR1* transcript, we found that TRV infection was correlated with the massive accumulation of degradome 5' signatures at nucleotide positions 156, 2219 and 2247 (Fig. 5b). These cleavage site sequences were clearly discerned from a background of low abundant, nonspecific degradation products at other positions (Fig. 5b). Cleavage at position 156 was reproducibly found with high abundance in all degradome libraries prepared from leaves or inflorescences of TRV-infected plants. Although this precise 5' signature was not found in mock-inoculated controls, degradome tags diagnostic of sequential cleavage were identified at nearby nucleotide positions in all samples tested, suggesting that this region was particularly prone to RNA degradation (Figs 5b, S6b). When we applied the CLEAVELAND4 computational pipeline to match *BIR1*-derived degradome 5' signatures against the miRBase, we were unable to identify validated miRNAs as potentially responsible for cleavage at these positions, suggesting that *BIR1*-derived siRNAs could guide *cis*-cleavage events. Collectively, our data proved that *BIR1* transcripts were exposed to selective post-transcriptional degradation in response to infection.

BIR1 overexpression causes extreme morphological defects and upregulation of plant defense in TRV-infected *Arabidopsis*

To further explore the relevance of *BIR1* regulation in infected plants, we investigated the consequences of *BIR1* overexpression

during TRV infection in *Arabidopsis*. To do this, we used TRV as a viral expression vector to overproduce *BIR1* in infected plants. We cloned an HA-tagged version of the *Arabidopsis BIR1* into pTRV2 and introduced it along with pTRV1 in *N. benthamiana* by *Agrobacterium*-mediated infiltration (Fig. 6a). Western blot assay using anti-HA antibody detected *BIR1* protein in systemically infected leaves (Fig. 6a). Interestingly, TRV-*BIR1* RNA accumulated in upper noninfiltrated leaves to the same degree as the TRV-GFP control, suggesting that overexpression of *BIR1* had negligible effects on TRV accumulation in *N. benthamiana* cells (Figs 6a, S6c).

Inoculation of 3-wk-old *Arabidopsis* plants with TRV-*BIR1* revealed the appearance of a range of morphological defects at *c.* 14 dpi, affecting >80% of the inoculated plants (Fig. 6b). Symptoms were more severe at later stages postinfection and included stunted morphology, abnormal leaf shape, extensive leaf necrosis, loss of apical dominance during bolting (bushy phenotype) and premature death (Fig. 6b). By contrast, plants infected with TRV-GFP, used as control, developed normally, like uninoculated or mock-inoculated plants (Fig. 6b). Interestingly, morphological phenotypes of TRV-*BIR1*-infected individual plants coincided with extremely high abundance of *BIR1* transcripts (Fig. 6c). Conversely, TRV-*BIR1*-infected plants that developed free of symptoms accumulated lower amounts of *BIR1* transcripts, similar to the TRV-GFP-infected control plants (Fig. 6c).

Growth arrest and cell death are reminiscent of plants that show constitutive activation of defense responses (Lorrain *et al.*, 2003). To gain an insight into the effects of *BIR1* overexpression in TRV-infected tissues, we measured relative transcript abundance of defense genes *PR1* and *PR4*. Despite *BIR1* being a repressor of plant immunity, the expression of *PR1* and *PR4* was markedly upregulated in the infected plants that produced high amounts of *BIR1* transcripts (Fig. 6d). By contrast, *PR1* and *PR4* accumulated to normal levels in symptomless plants that produced low amounts of *BIR1* transcripts (Fig. 6d). *PR1* and *PR4* were poorly induced in plants infected with TRV-GFP, confirming that defense activation was linked to *BIR1* overexpression rather than virus infection (Fig. 6d). These experiments suggested that *BIR1*

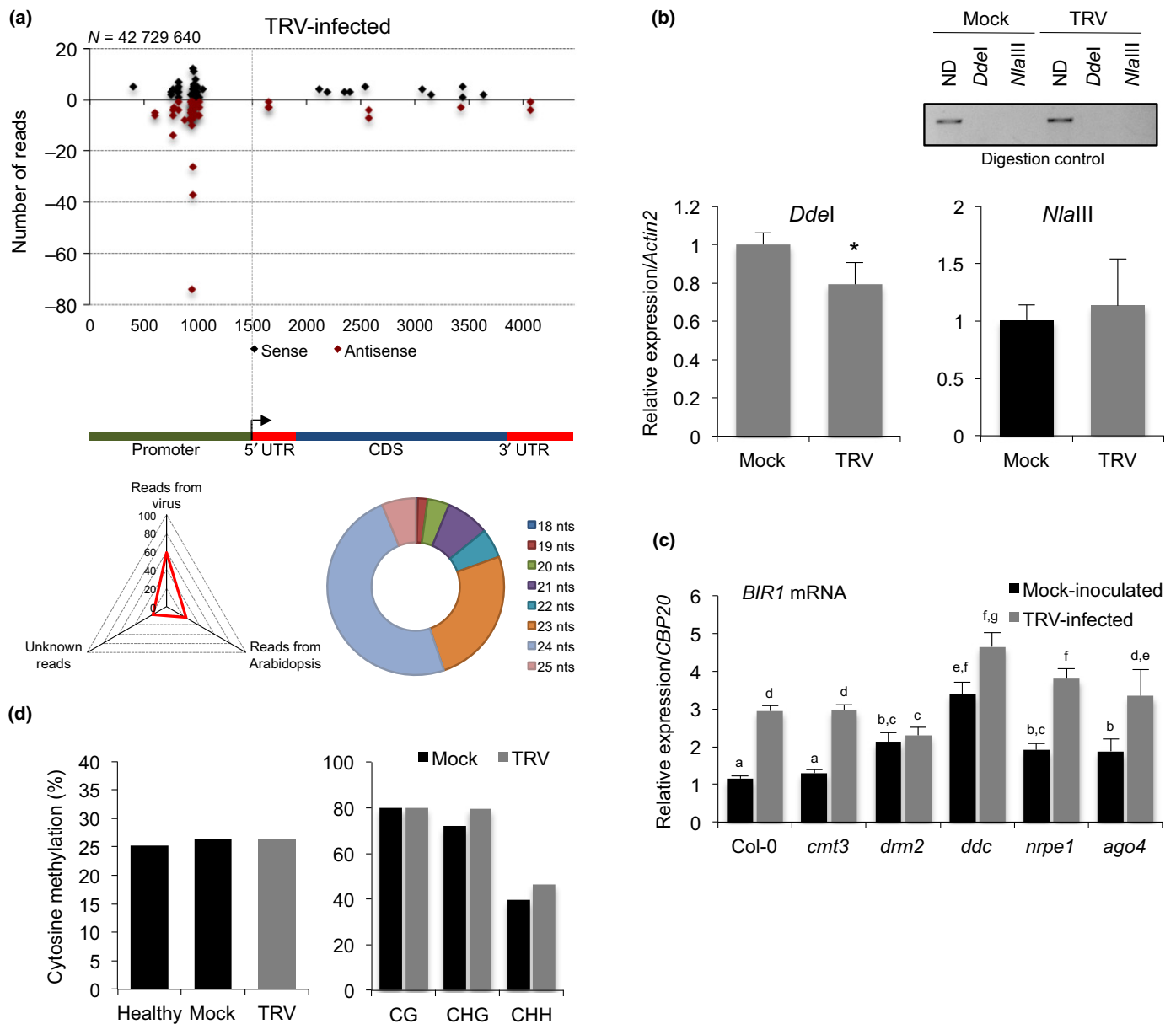


Fig. 4 *BIR1* methylation status in *Tobacco rattle virus* (TRV)-infected Arabidopsis. (a) Distribution of *BIR1*-derived small interfering RNAs (siRNAs) in rosette leaves of TRV-infected Arabidopsis plants. Sense (black dots) and antisense (red dots) siRNA species are represented as positive and negative values on the y-axis, respectively. The triangle graph represents the genomic distribution (percentage) of siRNAs in the sequenced set. *N* denotes the total number of filtered sequenced reads. The circle graph represents the size distribution of *BIR1*-derived siRNAs in TRV-infected plants. (b) Extent of asymmetric cytosine methylation at the *BIR1* promoter determined by Chop-qPCR in rosette leaves of mock-inoculated and TRV-infected plants at 8 d post-inoculation (dpi). The genomic DNA was digested with methylation-sensitive enzymes *DdeI* and *NlaIII* and qPCR-amplified. Nondigested (ND) plants were used as controls. Values were normalized to the *Actin2* internal control. Error bars represent SD from three independent biological replicates. (c) Accumulation of *BIR1* transcripts in rosette leaves of mock-inoculated and TRV-infected plants of wild-type (Col-0) and RNA-directed DNA methylation (RdDM) mutants (*cmt3*, *drm2*, *ddc*, *nrpe1* and *ago4*) at 8 dpi. Relative values were determined by quantitative reverse transcription polymerase chain reaction and normalized to the *CBP20* internal control. Error bars represent SD from three independent PCR measurements. (d) Percentage of total cytosine methylation (left) and nonCG DNA methylation, CHG and CHH methylation (right) determined by in-house bisulfite sequencing at the *BIR1* promoter in healthy (uninoculated), mock-inoculated and TRV-infected Arabidopsis at 8 dpi. H represents A, T or C. Asterisks (Student's *t*-test) or different letters (one-way ANOVA) were used to indicate significant differences ($P < 0.001$). The experiments were repeated at least three times with similar results, and one representative biological replicate is shown.

overexpression induces constitutive immunity in Arabidopsis. Interestingly, TRV levels in TRV-*BIR1*-infected plants exhibited a marked variability between individuals and experimental replicates (Fig. 6e), and no correlation between *BIR1*

transcript abundance and viral accumulation was found (bilateral Spearman correlation, $\rho = 0.48$, $P = 0.84$). We concluded that *BIR1* overexpression had no direct effects on viral susceptibility in Arabidopsis.

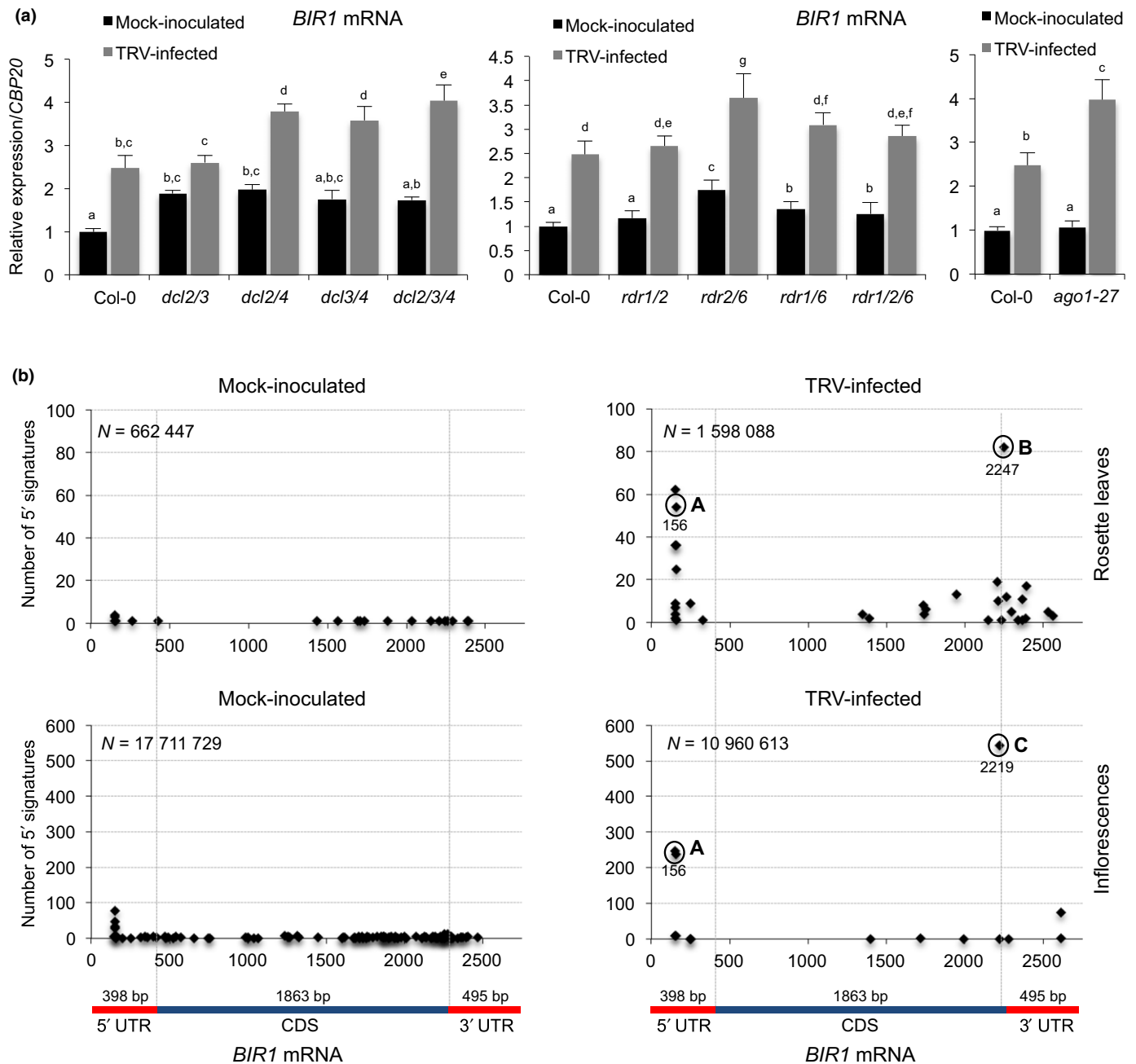
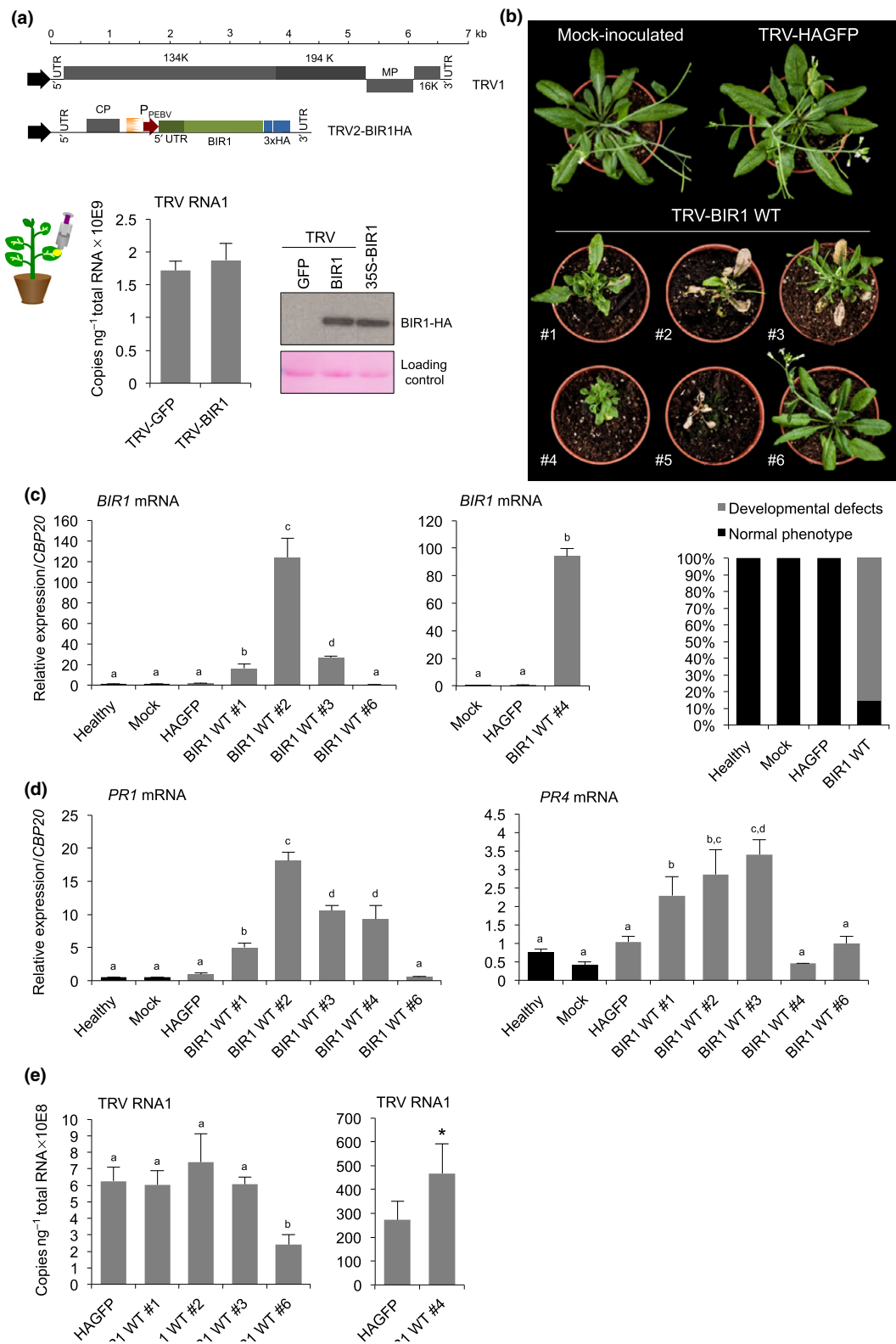


Fig. 5 *BIR1* mRNA accumulation in RNA-silencing mutants and parallel analysis of RNA ends-based identification of preferential cleavage sites within the *BIR1* mRNA. (a) Accumulation of *BIR1* transcripts in mock-inoculated and *Tobacco rattle virus* (TRV)-infected Arabidopsis rosette leaves of wild-type (Col-0) and mutants impaired in small interfering RNA (siRNA) biogenesis (*dcl2 dcl3* (*dcl2/3*), *dcl2 dcl4* (*dcl2/4*), *dcl3 dcl4* (*dcl3/4*) or *dcl2 dcl3 dcl4* (*dcl2/3/4*)), secondary siRNA biogenesis (*rdr1 rdr2* (*rdr1/2*), *rdr2 rdr6* (*rdr2/6*), *rdr1 rdr6* (*rdr1/6*) or *rdr1 rdr2 rdr6* (*rdr1/2/6*)), and AGO1 function (*ago1*). Relative expression levels were determined at 8 d post-inoculation (dpi) by quantitative reverse transcription polymerase chain reaction and normalized to the *CBP20* internal control. Error bars represent SD from three independent PCR measurements. Different letters indicate significant differences according to one-way ANOVA and Duncan test ($P < 0.001$). The experiments were repeated at least three times with similar results and one representative biological replicate is shown. (b) Target plots showing 5' signature abundance throughout the *BIR1* mRNA identified through degradome sequencing. Circles in the t-plots denote highly abundant signatures at the indicated positions (referred to as A, B and C) identified in TRV-infected plants but not in mock-inoculated controls. Samples from rosette leaves and inflorescences were analyzed. *N* denotes the total number of filtered sequenced reads.

Inducible *BIR1* overexpression in transgenic Arabidopsis causes phenotypic defects and triggers the activation of plant defense

It is possible that the morphological phenotypes associated with high *BIR1* doses in TRV-*BIR1*-infected cells were a result of the

combined effect of *BIR1* overexpression and viral infection. To further investigate this possibility, we employed a DEX-inducible system to generate independent Arabidopsis homozygous lines that overexpress mCherry-tagged *BIR1* proteins (Fig. S7a,b,c,d). DEX treatment had no apparent effects on wild-type Col-0 seedlings, and *BIR1* transgenics treated with water exhibited



normal phenotypes (Figs 7a, S8a,b). Conversely, > 80% of DEX-treated *BIR1* transgenics displayed stunting, abnormal leaf shape, leaf necrosis, bushy phenotype and cell death that resembled the morphological phenotypes observed in plants infected with TRV-BIR1 (Figs 7a, S8a,b). As predicted, DEX-treated plants

showing strong phenotypes accumulated over two orders of magnitude more *BIR1* transcripts than control plants (Fig. 7b). Water-treated transgenic lines, wild-type (nontransgenic) plants treated with DEX, and DEX-treated transgenics that exhibited normal growing phenotypes produced equivalent low amounts of

Fig. 6 Phenotypes of *Tobacco rattle virus* (TRV)-BIR1-infected *Arabidopsis*. (a) TRV-derived constructs for HA-tagged expression of BIR1. The 5' UTR-containing BIR1 coding sequence was inserted adjacent to the *Pea early browning virus* (PEBV) replicase promoter in pTRV2. pTRV1 and pTRV2-BIR1 constructs were agroinjected in *Nicotiana benthamiana*. Accumulation of TRV genomic RNA in upper leaves of TRV-BIR1-infected plants at 5 d postinoculation (dpi) is shown (left). Western blot analysis of HA-tagged BIR1 proteins in extracts from leaves infiltrated with TRV-BIR1 is shown (right). TRV-green fluorescent protein (TRV-GFP) and 35S-BIR1-HA were used as controls. Ponceau staining was used as a protein loading control. (b) Morphological phenotypes of mock-inoculated plants, those systemically infected with TRV-GFP or infected with TRV-BIR1 wild-type (WT, referred to as #1 to #6). Plants were grown on soil and photographed at 14 dpi. The percentage of plants displaying normal vs morphological phenotypes after inoculation with TRV derivatives is indicated. Uninoculated (healthy) and mock-inoculated plants were used as controls. TRV-GFP was used as a control. (c) Accumulation of *BIR1* transcripts in TRV-BIR1-infected individual plants shown in (b). Samples from uninoculated (healthy), mock-inoculated or TRV-GFP-infected plants were included as controls. (d) Accumulation of defense-related *PR1* and *PR4* transcripts in TRV-BIR1-infected individual plants shown in (b). TRV-GFP was used as a control. (e) Accumulation of TRV genomic RNA in TRV-BIR1-infected individual plants shown in (b). Relative expression levels were determined by quantitative reverse transcription polymerase chain reaction and normalized to the *CBP20* internal control. Error bars represent SD from three independent PCR measurements. Asterisks (Student's *t*-test) or different letters (one-way ANOVA) were used to indicate significant differences ($P < 0.001$). The experiments were repeated at least three times with similar results, and one representative biological replicate is shown.

BIR1 transcripts (Fig. 7b). Similarly, BIR1-mCherry fusion proteins were detected at much higher intensities in plants with morphological defects than in the controls (Fig. 7c).

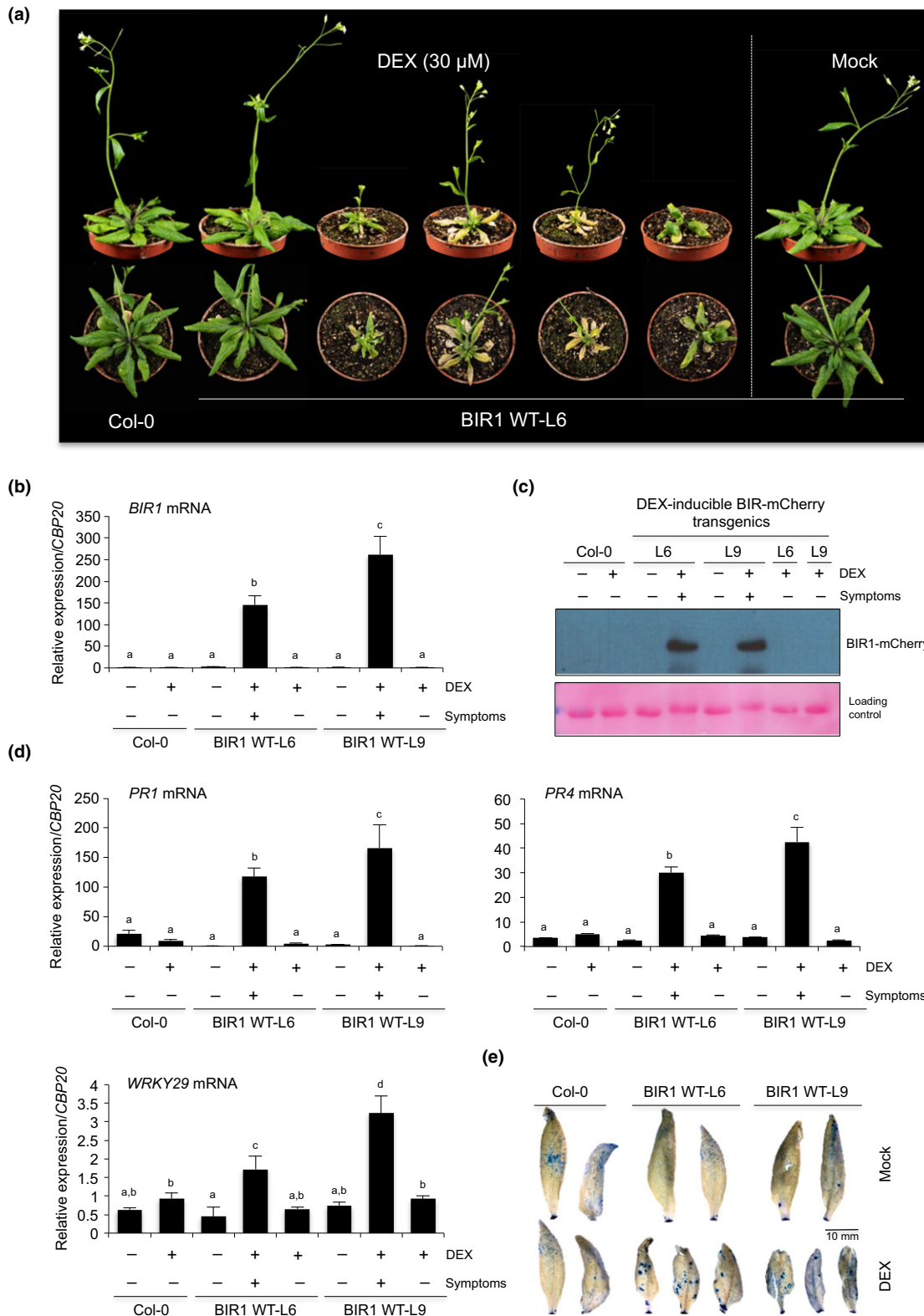
When the accumulation of defense gene markers was tested, high amounts of *PR1*, *PR4*, *PAD3* or *WRKY29* transcripts accumulated in plants overexpressing *BIR1* as opposed to wild-type or nonexpressing transgenic plants (Figs 7d, S8c). As predicted, none of these markers was upregulated in asymptomatic *BIR1* transgenics (Figs 7d, S8c). We further demonstrated that overexpression of *BIR1* triggered localized cell death in DEX-treated transgenic leaves, as deduced by trypan blue staining (Fig. 7e). These observations indicated that DEX-induced overexpression of *BIR1* stimulated an autoimmune response in an infection-free cell environment.

Discussion

BIR1 is a negative regulator of several resistance pathways in which BAK1 and SOBIR1 have concerted roles (Gao *et al.*, 2009; Dominguez-Ferreras *et al.*, 2015; Liu *et al.*, 2016). Here we provide compelling evidence that *BIR1* transcription is positively regulated by SA and propose that TRV triggers NPR1-dependent expression of *BIR1* during the infection by increasing SA concentrations in the infected tissue. We show that loss of BIR1 function in the *bir1-1* mutant severely compromises TRV accumulation, probably as a result of constitutive activation of plant defenses in this mutant. A previous study reported that the *bir1-1* mutation leads to extensive cell death, elevated concentrations of SA and SA-dependent gene expression (Gao *et al.*, 2009). Based on this observation, it is possible that the SA defense pathway could prime an immune response against TRV in *bir1-1* mutants. In some compatible plant–virus interactions, SA treatment or overexpression of SA biosynthetic genes can potentiate antiviral responses by affecting virus replication, coat protein accumulation and systemic virus movement (Chivasa *et al.*, 1997; Mayers *et al.*, 2005; Ishihara *et al.*, 2008; Qi *et al.*, 2018). However, we found that exogenous application of SA activated the SA defense pathway but was unable to antagonize the virus. Furthermore, a phenotype of strong resistance against TRV was also observed in the double *bir1-1 sobir1-1* mutant, in which cell death and constitutive expression of SA-dependent defense genes are strongly reduced by the *sobir1-1* mutation (Gao *et al.*, 2009).

These findings prove that enhanced TRV resistance in *bir1-1* plants was not a result of constitutive SA defense priming (Gao *et al.*, 2009). On the contrary, we observed that loss of ICS1 function in the *sid2-2* mutants was correlated with reduced TRV proliferation, suggesting that SA may be important to support TRV infection. Importantly, altered susceptibility was not observed in plants expressing high levels of BIR1, even though cell death and SA-mediated defense signaling pathway were substantially enhanced in BIR1 overexpressor plants. These results suggest that defense responses that were concomitant to both low and high expression of *BIR1* may have a minor role in controlling viral proliferation in *Arabidopsis*. BAK1 is also required for activation of cell death and defense responses in the *bir1-1* mutant (Liu *et al.*, 2016). We show that *BAK1* transcripts were diminished in infected plants, and that *bak1-5* mutants, which are impaired in PTI but not in BR signaling (Chinchilla *et al.*, 2007; Heese *et al.*, 2007; Schwessinger *et al.*, 2011), were more susceptible to infection with TRV and other viruses (Korner *et al.*, 2013). These findings suggest that BAK1, and probably SOBIR1, contribute to modulate viral proliferation, but their relationships with BIR1 and their potential interdependence during the antiviral response remain to be investigated. Furthermore, the role of NDR1-, PAD4- and EDS1-resistance pathways that are triggered in the *bir1-1* mutant needs to be investigated to elucidate their contribution to antiviral resistance (Gao *et al.*, 2009).

In our study, we prove that both transcriptional and post-transcriptional RNA silencing contribute, at least partly, to *BIR1* homeostasis. We found that RdDM constitutively regulates *BIR1*. Under nonchallenging conditions, our results suggest that post-transcriptional silencing may be mobilized to perform conditional fine-tuned regulation of *BIR1* expression. However, during viral infection, post-transcriptional silencing strongly reinforces the action of epigenetic silencing by removing the excess of *BIR1* transcripts produced upon *BIR1* transcriptional activation. This idea also emerges from our analysis of degradome according to which *BIR1* gives rise to high amounts of discrete cleaved 3' mRNA products in infected plants compared with mock-inoculated plants. The genetic requirement for RNA silencing components in the control of *BIR1* is consistent with the widespread accumulation of *BIR1*-derived siRNAs of sense and antisense polarities in infected plants, but not in mock-inoculated ones. *BIR1* siRNAs resemble viral-associated siRNAs



(vasiRNAs) that are produced from multiple host genes during activation of antiviral silencing (Cao *et al.*, 2014). vasiRNAs are competent in directing silencing of the host target genes in line with the idea that *BIR1* siRNAs may guide autosilencing of *BIR1*

transcripts. The requirement for *BIR1* siRNA biogenesis and function seems to differ, however, from the predicted genetic pathway of vasiRNAs, which are mostly dependent on DCL4, RDR1 and AGO2 (Cao *et al.*, 2014). From our data, it is

Fig. 7 Phenotypes of *BIR1*-overexpressing transgenic Arabidopsis. (a) Morphological phenotypes of *BIR1* transgenic plants after dexamethasone (DEX) treatment. Arabidopsis plants from transgenic line 6 (*BIR1* wild-type (WT) L6) were grown for 3 wk on soil and treated with 30 μ M DEX or mock-treated for 6 d consecutively by spraying the solution (1 ml per plant) once at 24 h intervals. DEX-treated wild-type (Col-0) plants are shown as controls. Plants were photographed at 7 d after the first DEX application. Morphological phenotypes of plants from transgenic line 9 (L9) are shown in Supporting Information Fig. S8(a). (b) Accumulation of *BIR1* transcripts in plants from *BIR1* overexpressor lines L6 and L9. WT plants are shown as controls. Plants were sprayed with DEX (+) or water (-). Plants showing WT (-) or aberrant (+) phenotypes were analyzed. (c) Western blot analysis of *BIR1* proteins in extracts from leaves of lines L6 and L9. Plants were sprayed with DEX (+) or water (-). Plants showing WT (-) or aberrant (+) phenotypes were analyzed. Ponceau staining was used as a protein loading control. (d) Accumulation of defense-related *PR1*, *PR4*, and *PAD3* transcripts in plants from lines L6 and L9. (e) Trypan blue staining of leaves of WT and *BIR1* overexpression lines (L6 and L9). Leaves from DEX-treated and mock-treated plants grown on soil were stained with lactophenol trypan blue as previously described (Diaz-Tielas *et al.*, 2012). Relative expression levels were determined by quantitative reverse transcription polymerase chain reaction and normalized to the *CBP20* internal control. Error bars represent SD from three independent PCR measurements. Different letters indicate significant differences according to one-way ANOVA and Duncan test ($P < 0.001$). The experiments were repeated at least three times with similar results, and one representative biological replicate is shown.

possible that several complementary pathways that include RDR6 and AGO1 also contribute to vasiRNA biogenesis and function during viral infections.

We found that the strong overexpression of *BIR1* triggers autoimmune phenotypes similar to those observed in *bir1-1* mutants (Gao *et al.*, 2009), indicating that a well-calibrated regulation of *BIR1* guarantees a proper control of immune signaling pathways. Given that *BIR1* is an active RLKs, overexpression of *BIR1* may interfere with other closely related RLKs causing miscoordination of cellular signaling pathways, including plant defense or development. In line with this scenario, overproduction of *BIR1* may either affect *BIR1*-dependent negative regulation of (co)receptor partners or, alternatively, promote inappropriate interactions with other immune (co)receptor proteins that result in the activation of resistance (Prelich, 2012; Rodriguez *et al.*, 2016). For instance, high levels of *BIR1* may hinder BAK1-mediated regulation of SOBIR1-independent cell death (Liu *et al.*, 2016).

We saw that Arabidopsis mutants with defects in RdDM or siRNA biogenesis/function produce *BIR1* at levels that barely compromise normal plant development. This finding has two important implications. First, one could argue that RNA silencing plays a secondary role in controlling *BIR1* expression and that other yet unknown mechanisms provide additional layers of regulation that ultimately confine *BIR1* below detrimental levels for plant fitness. This is a reasonable possibility, but loss of function of one or several silencing genes does not necessarily imply a complete inhibition of the pathway (Bouche *et al.*, 2006). And importantly, mutants tested in this study were affected either in the RdDM pathway or in the post-transcriptional silencing pathway, but not both. As a result, it is likely that residual RNA-silencing activities in these mutants could yet exert effective *BIR1* control, preventing *BIR1* from reaching deleterious expression levels upon virus or pathogen (SA-mediated) induction. The second implication is that phenotypes associated with *BIR1* induction are probably dose-dependent. In our experiments, plants infected with TRV-*BIR1* or DEX-treated transgenic plants showing developmental defects produced *BIR1* transcripts that were more than two orders of magnitude higher than those in control plants. Conversely, we observed that seedlings of the same transgenic lines developed normally when they were grown on MS-DEX plates (Fig. S9a). In these experimental conditions, transgenic plants accumulated only 10–20 times more *BIR1*

transcripts than the wild-type plants (Fig. S9b). This represented an expression level at least an order of magnitude lower than that observed in DEX-treated, soil-grown plants. Furthermore, accumulation of defense genes was not substantially altered in transgenic seedlings (lines 5 and 6) grown on plates (Fig. S9c). Only, transgenic line 9 produced *BIR1* transcripts at levels that triggered a modest induction of *PR1*, *PR4* and *PAD3*, but they were insufficient to perturb normal development (Fig. S9c). A dose-dependent mechanism would explain why silencing mutants, in which increments in *BIR1* expression were only mild, display normal phenotypes. Interestingly, *ddc* mutants show a suite of developmental abnormalities (Chan *et al.*, 2006) and activation of defense genes (Fig. S9d) (Downen *et al.*, 2012), but morphological phenotypes in these plants are probably a result of a broad misregulation of developmental genes that are normally controlled by nonCG methylation (Chan *et al.*, 2006). *BIR1* belongs to the *BIR* family, with four members, including *BIR2* and *BIR3*, that also function as negative regulators of BAK1-mediated immunity (Halter *et al.*, 2014; Imkampe *et al.*, 2017). Transgenic overexpression of *BIR3* in Arabidopsis also leads to dwarf phenotypes that were dosage-dependent (Imkampe *et al.*, 2017). From our experiments, we conclude that regulation of *BIR1* is critical for plant viability, and propose that proper *BIR1* functioning requires a threshold expression, and once *BIR1* exceeds or falls behind such a threshold, misregulation of plant immunity takes place. Interestingly, in a previous study, *BIR1* transgenic Arabidopsis under a 35S promoter exhibited wild-type morphology, and PTI responses were apparently unaffected in these plants, suggesting that the *BIR1* transgene was expressed at nondetrimental levels in their experimental conditions (Liu *et al.*, 2016).

In conclusion, our results demonstrate that plant viruses initiate a basal immune response that involves SA-dependent activation of the immune repressor *BIR1*. We propose that *BIR1* acts as a negative regulator of antiviral defense in Arabidopsis. Regulation of *BIR1* gene expression is important to avoid constitutive defense responses that negatively impact plant development and fitness. In this scenario, RNA silencing provides two complementary layers of transcriptional and post-transcriptional regulation that prevent, alone or in conjunction with other regulatory mechanisms, *BIR1* from reaching deleterious expression levels when *BIR1* is transcriptionally activated (Fig. S10a,b). Our work provides novel mechanistic insights into the regulation of *BIR1* homeostasis that may be common for other plant immune components.









Acknowledgements

This work has been supported by FPI fellowships (BES-2013-063138 and EEBB-I-16-10815) to IG-B, by a Ramon y Cajal grant (RyC-2011-07006) to VR-F and by National Research grants (BIO2012-39973 and BIO2015-70752-R) to CL from Ministerio de Economía y Competitividad (MINECO/FEDER), Spain, and by a National Institutes of Health (USA) grant R01GM108722 to ATW. We thank Yuelin Zhang, James Carington, Steve Jacobsen, Craig Pikaard, Xinning Dong and Eric Richards for providing seeds, and Ignacio Hamada, Jan Kuciński, Shriya Sethuraman and M. Hafiz Rothi for technical assistance.

Author contributions

CL conceived and designed the study; IG-B, LD, ATW and CL outlined experiments; IG-B, LD, VA-S, JGV, AE, VR-F and CL performed research; LD and CL contributed with computer analysis; IG-B, LD, ATW and CL analyzed data; and CL wrote the paper.

ORCID

Vítor Amorim-Silva  <https://orcid.org/0000-0002-3978-7205>
 Livia Donaïre  <https://orcid.org/0000-0002-5454-2994>
 Alicia Esteban  <https://orcid.org/0000-0003-3039-1172>
 Irene Guzmán-Benito  <https://orcid.org/0000-0002-9912-8164>
 César Llave  <https://orcid.org/0000-0003-3844-4582>
 Virginia Ruiz-Ferrer  <https://orcid.org/0000-0002-7840-297X>
 José G. Vallarino  <https://orcid.org/0000-0002-0374-8706>
 Andrzej T. Wierzbicki  <https://orcid.org/0000-0002-5713-1306>

References

- Addo-Quaye C, Miller W, Axtell MJ. 2009. CleaveLand: a pipeline for using degradome data to find cleaved small RNA targets. *Bioinformatics* 25: 130–131.
- Boccardo M, Sarazin A, Thiebaud O, Jay F, Voïnet O, Navarro L, Colot V. 2014. The *Arabidopsis* miR472-RDR6 silencing pathway modulates PAMP- and effector-triggered immunity through the post-transcriptional control of disease resistance genes. *PLoS Pathogens* 10: e1003883.
- Bohmdorfer G, Rowley MJ, Kucinski J, Zhu Y, Amies I, Wierzbicki AT. 2014. RNA-directed DNA methylation requires stepwise binding of silencing factors to long non-coding RNA. *The Plant Journal* 79: 181–191.
- Bohmdorfer G, Sethuraman S, Rowley MJ, Krzysztan M, Rothi MH, Bouzit L, Wierzbicki AT. 2016. Long non-coding RNA produced by RNA polymerase V determines boundaries of heterochromatin. *eLife* 5: e19092.
- Boller T, Felix G. 2009. A renaissance of elicitors: perception of microbe-associated molecular patterns and danger signals by pattern-recognition receptors. *Annual Review of Plant Biology* 60: 379–406.
- Bouche N, Laressesgues D, Gascioli V, Vaucheret H. 2006. An antagonistic function for *Arabidopsis* DCL2 in development and a new function for DCL4 in generating viral siRNAs. *EMBO Journal* 25: 3347–3356.
- Campo S, Peris-Peris C, Sire C, Moreno AB, Donaïre L, Zytnicki M, Notredame C, Llave C, San Segundo B. 2013. Identification of a novel microRNA (miRNA) from rice that targets an alternatively spliced transcript of the *Nramp6* (Natural resistance-associated macrophage protein 6) gene involved in pathogen resistance. *New Phytologist* 199: 212–227.
- Cao H, Glazebrook J, Clarke JD, Volko S, Dong X. 1997. The *Arabidopsis* *NPRI* gene that controls systemic acquired resistance encodes a novel protein containing ankyrin repeats. *Cell* 88: 57–63.
- Cao M, Du P, Wang X, Yu YQ, Qiu YH, Li W, Gal-On A, Zhou C, Li Y, Ding SW. 2014. Virus infection triggers widespread silencing of host genes by a distinct class of endogenous siRNAs in *Arabidopsis*. *Proceedings of the National Academy of Sciences, USA* 111: 14613–14618.
- Cao X, Jacobsen SE. 2002. Locus-specific control of asymmetric and CpNpG methylation by the *DRM* and *CMT3* methyltransferase genes. *Proceedings of the National Academy of Sciences, USA* 99(Suppl 4): 16491–16498.
- Chan SW, Henderson IR, Zhang X, Shah G, Chien JS, Jacobsen SE. 2006. RNAi, DRD1, and histone methylation actively target developmentally important non-CG DNA methylation in *Arabidopsis*. *PLoS Genetics* 2: e83.
- Chen Z, Zheng Z, Huang J, Lai Z, Fan B. 2009. Biosynthesis of salicylic acid in plants. *Plant Signaling & Behavior* 4: 493–496.
- Chinchilla D, Zipfel C, Robatzek S, Kemmerling B, Nurnberger T, Jones JD, Felix G, Boller T. 2007. A flagellin-induced complex of the receptor FLS2 and BAK1 initiates plant defence. *Nature* 448: 497–500.
- Chivasa S, Murphy AM, Naylor M, Carr JP. 1997. Salicylic acid interferes with *Tobacco Mosaic Virus* replication via a novel salicylhydroxamic acid-sensitive mechanism. *Plant Cell* 9: 547–557.
- Clough SJ, Bent AF. 1998. Floral dip: a simplified method for *Agrobacterium*-mediated transformation of *Arabidopsis thaliana*. *The Plant Journal* 16: 735–743.
- Coll NS, Epple P, Dangl JL. 2011. Programmed cell death in the plant immune system. *Cell Death and Differentiation* 18: 1247–1256.
- Dangl JL, Jones JD. 2001. Plant pathogens and integrated defence responses to infection. *Nature* 411: 826–833.
- Diaz-Tielas C, Grana E, Sotelo T, Reigosa MJ, Sanchez-Moreiras AM. 2012. The natural compound trans-chalcone induces programmed cell death in *Arabidopsis thaliana* roots. *Plant, Cell & Environment* 35: 1500–1517.
- Dodds PN, Rathjen JP. 2010. Plant immunity: towards an integrated view of plant-pathogen interactions. *Nature Reviews Genetics* 11: 539–548.
- Dominguez-Ferreras A, Kiss-Papp M, Jehle AK, Felix G, Chinchilla D. 2015. An overdose of the *Arabidopsis* coreceptor BRASSINOSTEROID INSENSITIVE1-ASSOCIATED RECEPTOR KINASE1 or its ectodomain causes autoimmunity in a SUPPRESSOR OF BIR1-1-dependent manner. *Plant Physiology* 168: 1106–1121.
- Donaïre L, Pedrola L, de la Rosa R, Llave C. 2011. High-throughput sequencing of RNA silencing-associated small RNAs in olive (*Olea europaea* L.). *PLoS ONE* 6: e27916.
- Downen RH, Pelizzola M, Schmitz RJ, Lister R, Downen JM, Nery JR, Dixon JE, Ecker JR. 2012. Widespread dynamic DNA methylation in response to biotic stress. *Proceedings of the National Academy of Sciences, USA* 109: E2183–E2191.
- Fernandez-Calvino L, Guzman-Benito I, Del Toro FJ, Donaïre L, Castro-Sanz AB, Ruiz-Ferrer V, Llave C. 2016a. Activation of senescence-associated *Dark-inducible (DIN)* genes during infection contributes to enhanced susceptibility to plant viruses. *Molecular Plant Pathology* 17: 3–15.
- Fernandez-Calvino L, Martinez-Priego L, Szabo EZ, Guzman-Benito I, Gonzalez I, Canto T, Lakatos L, Llave C. 2016b. *Tobacco rattle virus* 16K silencing suppressor binds ARGONAUTE 4 and inhibits formation of RNA silencing complexes. *Journal of General Virology* 97: 246–257.
- Fernandez-Calvino L, Osorio S, Hernandez ML, Hamada IB, Del Toro FJ, Donaïre L, Yu A, Bustos R, Fernie AR, Martinez-Rivas JM *et al.* 2014. Virus-induced alterations in primary metabolism modulate susceptibility to *Tobacco rattle virus* in *Arabidopsis*. *Plant Physiology* 166: 1821–1838.
- Gao M, Wang X, Wang D, Xu F, Ding X, Zhang Z, Bi D, Cheng YT, Chen S, Li X *et al.* 2009. Regulation of cell death and innate immunity by two receptor-like kinases in *Arabidopsis*. *Cell Host & Microbe* 6: 34–44.
- German MA, Luo S, Schroth G, Meyers BC, Green PJ. 2009. Construction of parallel analysis of RNA ends (PARE) libraries for the study of cleaved miRNA targets and the RNA degradome. *Nature Protocols* 4: 356–362.
- German MA, Pillay M, Jeong DH, Hetawal A, Luo S, Janardhanan P, Kannan V, Rymarquis LA, Nobuta K, German R *et al.* 2008. Global identification of microRNA-target RNA pairs by parallel analysis of RNA ends. *Nature Biotechnology* 26: 941–946.

- Gouveia BC, Calil IP, Machado JP, Santos AA, Fontes EP. 2016. Immune receptors and co-receptors in antiviral innate immunity in plants. *Frontiers in Microbiology* 7: 2139.
- Halter T, Imkamp J, Mazzotta S, Wierzba M, Postel S, Bucherl C, Kiefer C, Stahl M, Chinchilla D, Wang X *et al.* 2014. The leucine-rich repeat receptor kinase BIR2 is a negative regulator of BAK1 in plant immunity. *Current Biology* 24: 134–143.
- He XF, Fang YY, Feng L, Guo HS. 2008. Characterization of conserved and novel microRNAs and their targets, including a TuMV-induced TIR-NBS-LRR class R gene-derived novel miRNA in *Brassica*. *FEBS Letters* 582: 2445–2452.
- He XJ, Hsu YF, Pontes O, Zhu J, Lu J, Bressan RA, Pikaard C, Wang CS, Zhu JK. 2009. NRPD4, a protein related to the RPB4 subunit of RNA polymerase II, is a component of RNA polymerases IV and V and is required for RNA-directed DNA methylation. *Genes & Development* 23: 318–330.
- Heese A, Hann DR, Gimenez-Ibanez S, Jones AM, He K, Li J, Schroeder JI, Peck SC, Rathjen JP. 2007. The receptor-like kinase SERK3/BAK1 is a central regulator of innate immunity in plants. *Proceedings of the National Academy of Sciences, USA* 104: 12217–12222.
- Imkamp J, Halter T, Huang S, Schulze S, Mazzotta S, Schmidt N, Manstretta R, Postel S, Wierzba M, Yang Y *et al.* 2017. The *Arabidopsis* leucine-rich repeat receptor kinase BIR3 negatively regulates BAK1 receptor complex formation and stabilizes BAK1. *Plant Cell* 29: 2285–2303.
- Ishihara T, Sekine KT, Hase S, Kanayama Y, Seo S, Ohashi Y, Kusano T, Shibata D, Shah J, Takahashi H. 2008. Overexpression of the *Arabidopsis thaliana* EDS5 gene enhances resistance to viruses. *Plant Biology (Stuttgart, Germany)* 10: 451–461.
- Johansen LK, Carrington JC. 2001. Silencing on the spot. Induction and suppression of RNA silencing in the *Agrobacterium*-mediated transient expression system. *Plant Physiology* 126: 930–938.
- Jones JD, Dangl JL. 2006. The plant immune system. *Nature* 444: 323–329.
- Katiyar-Agarwal S, Gao S, Vivian-Smith A, Jin H. 2007. A novel class of bacteria-induced small RNAs in *Arabidopsis*. *Genes & Development* 21: 3123–3134.
- Katiyar-Agarwal S, Morgan R, Dahlbeck D, Borsani O, Villegas A Jr, Zhu JK, Staskawicz BJ, Jin H. 2006. A pathogen-inducible endogenous siRNA in plant immunity. *Proceedings of the National Academy of Sciences, USA* 103: 18002–18007.
- Korner CJ, Klauser D, Niehl A, Dominguez-Ferreras A, Chinchilla D, Boller T, Heinlein M, Hann DR. 2013. The immunity regulator BAK1 contributes to resistance against diverse RNA viruses. *Molecular Plant–Microbe Interactions* 26: 1271–1280.
- Lellis AD, Kasschau KD, Whitham SA, Carrington JC. 2002. Loss-of-susceptibility mutants of *Arabidopsis thaliana* reveal an essential role for eIF(iso)4E during potyvirus infection. *Current Biology* 12: 1046–1051.
- Li F, Pignatta D, Bendix C, Brunkard JO, Cohn MM, Tung J, Sun H, Kumar P, Baker B. 2012. MicroRNA regulation of plant innate immune receptors. *Proceedings of the National Academy of Sciences, USA* 109: 1790–1795.
- Li Y, Lu YG, Shi Y, Wu L, Xu YJ, Huang F, Guo XY, Zhang Y, Fan J, Zhao JQ *et al.* 2014. Multiple rice microRNAs are involved in immunity against the blast fungus *Magnaporthe oryzae*. *Plant Physiology* 164: 1077–1092.
- Li Y, Zhang Q, Zhang J, Wu L, Qi Y, Zhou JM. 2010. Identification of microRNAs involved in pathogen-associated molecular pattern-triggered plant innate immunity. *Plant Physiology* 152: 2222–2231.
- Liu Y, Huang X, Li M, He P, Zhang Y. 2016. Loss-of-function of *Arabidopsis* receptor-like kinase BIR1 activates cell death and defense responses mediated by BAK1 and SOBIR1. *New Phytologist* 212: 637–645.
- Liu Y, Schiff M, Marathe R, Dinesh-Kumar SP. 2002. Tobacco *Rar1*, *EDS1* and *NPR1/NIM1* like genes are required for N-mediated resistance to *Tobacco mosaic virus*. *The Plant Journal* 30: 415–429.
- Lopez Sanchez A, Stassen JH, Furci L, Smith LM, Ton J. 2016. The role of DNA (de)methylation in immune responsiveness of *Arabidopsis*. *The Plant Journal* 88: 361–374.
- Lorrain S, Vaillau F, Balague C, Roby D. 2003. Lesion mimic mutants: keys for deciphering cell death and defense pathways in plants? *Trends in Plant Science* 8: 263–271.
- Ma C, Liu Y, Bai B, Han Z, Tang J, Zhang H, Yaghmaiean H, Zhang Y, Chai J. 2017. Structural basis for BIR1-mediated negative regulation of plant immunity. *Cell Research* 27: 1521–1524.
- Marques-Bueno MDM, Morao AK, Cayrel A, Platre MP, Barberon M, Caillieux E, Colot V, Jaillais Y, Roudier F, Vert G. 2016. A versatile Multisite Gateway-compatible promoter and transgenic line collection for cell type-specific functional genomics in *Arabidopsis*. *The Plant Journal* 85: 320–333.
- Martin GB, Bogdanove AJ, Sessa G. 2003. Understanding the functions of plant disease resistance proteins. *Annual Review of Plant Biology* 54: 23–61.
- Mayers CN, Lee KC, Moore CA, Wong SM, Carr JP. 2005. Salicylic acid-induced resistance to *Cucumber mosaic virus* in squash and *Arabidopsis thaliana*: contrasting mechanisms of induction and antiviral action. *Molecular Plant–Microbe Interactions* 18: 428–434.
- Meyers BC, Kozik A, Griego A, Kuang H, Michelmore RW. 2003. Genome-wide analysis of NBS-LRR-encoding genes in *Arabidopsis*. *Plant Cell* 15: 809–834.
- Navarro L, Dunoyer P, Jay F, Arnold B, Dharmasiri N, Estelle M, Voinnet O, Jones JD. 2006. A plant miRNA contributes to antibacterial resistance by repressing auxin signaling. *Science* 312: 436–439.
- Navarro L, Jay F, Nomura K, He SY, Voinnet O. 2008. Suppression of the microRNA pathway by bacterial effector proteins. *Science* 321: 964–967.
- Nicaise V, Candresse T. 2017. *Plum pox virus* capsid protein suppresses plant pathogen-associated molecular pattern (PAMP)-triggered immunity. *Molecular Plant Pathology* 18: 878–886.
- Ouyang S, Park G, Atamian HS, Han CS, Stajich JE, Kaloshian I, Borkovich KA. 2014. MicroRNAs suppress NB domain genes in tomato that confer resistance to *Fusarium oxysporum*. *PLoS Pathogens* 10: e1004464.
- Patterson K, Molloy L, Qu W, Clark S. 2011. DNA methylation: bisulphite modification and analysis. *Journal of Visualized Experiments: JoVE* 56: 3170.
- Prelich G. 2012. Gene overexpression: uses, mechanisms, and interpretation. *Genetics* 190: 841–854.
- Qi G, Chen J, Chang M, Chen H, Hall K, Korin J, Liu F, Wang D, Fu ZQ. 2018. Pandemonium breaks out: disruption of salicylic acid-mediated defense by plant pathogens. *Molecular Plant* 11: 1427–1439.
- Rodriguez E, El Ghouh H, Mundy J, Petersen M. 2016. Making sense of plant autoimmunity and ‘negative regulators’. *FEBS Journal* 283: 1385–1391.
- Rowley MJ, Avrutsky MI, Sifuentes CJ, Pereira L, Wierzbicki AT. 2011. Independent chromatin binding of ARGONAUTE4 and SPT5L/KTF1 mediates transcriptional gene silencing. *PLoS Genetics* 7: e1002120.
- Schwessinger B, Roux M, Kadota Y, Ntoukakis V, Sklenar J, Jones A, Zipfel C. 2011. Phosphorylation-dependent differential regulation of plant growth, cell death, and innate immunity by the regulatory receptor-like kinase BAK1. *PLoS Genetics* 7: e1002046.
- Shivaprasad PV, Chen HM, Patel K, Bond DM, Santos BA, Baulcombe DC. 2012. A microRNA superfamily regulates nucleotide binding site-leucine-rich repeats and other mRNAs. *Plant Cell* 24: 859–874.
- Stroud H, Greenberg MV, Feng S, Bernatavichute YV, Jacobsen SE. 2013. Comprehensive analysis of silencing mutants reveals complex regulation of the *Arabidopsis* methylome. *Cell* 152: 352–364.
- Takahashi Y, Nasir KH, Ito A, Kanzaki H, Matsumura H, Saitoh H, Fujisawa S, Kamoun S, Terauchi R. 2007. A high-throughput screen of cell-death-inducing factors in *Nicotiana benthamiana* identifies a novel MAPKK that mediates INF1-induced cell death signaling and non-host resistance to *Pseudomonas cichorii*. *The Plant Journal* 49: 1030–1040.
- Tena G, Boudsocq M, Sheen J. 2011. Protein kinase signaling networks in plant innate immunity. *Current Opinion in Plant Biology* 14: 519–529.
- Vallarino JG, Osorio S. 2016. Simultaneous determination of plant hormones by GC-TOF-MS. *Methods in Molecular Biology* 1363: 229–237.
- Wierzbicki AT, Cocklin R, Mayampurath A, Lister R, Rowley MJ, Gregory BD, Ecker JR, Tang H, Pikaard CS. 2012. Spatial and functional relationships among Pol V-associated loci, Pol IV-dependent siRNAs, and cytosine methylation in the *Arabidopsis* epigenome. *Genes & Development* 26: 1825–1836.
- Wildermuth MC, Dewdney J, Wu G, Ausubel FM. 2001. Isochorismate synthase is required to synthesize salicylic acid for plant defence. *Nature* 414: 562–565.

- Wu Y, Zhang D, Chu JY, Boyle P, Wang Y, Brindle ID, De Luca V, Despres C. 2012. The *Arabidopsis* NPR1 protein is a receptor for the plant defense hormone salicylic acid. *Cell Reports* 1: 639–647.
- Xiao YL, Redman JC, Monaghan EL, Zhuang J, Underwood BA, Moskal WA, Wang W, Wu HC, Town CD. 2010. High throughput generation of promoter reporter (GFP) transgenic lines of low expressing genes in *Arabidopsis* and analysis of their expression patterns. *Plant Methods* 6: 18.
- Xie M, Yu B. 2015. siRNA-directed DNA methylation in plants. *Current Genomics* 16: 23–31.
- Yi H, Richards EJ. 2007. A cluster of disease resistance genes in *Arabidopsis* is coordinately regulated by transcriptional activation and RNA silencing. *Plant Cell* 19: 2929–2939.
- Yu A, Lepere G, Jay F, Wang J, Bapaume L, Wang Y, Abraham AL, Penterman J, Fischer RL, Voinnet O *et al.* 2013. Dynamics and biological relevance of DNA demethylation in *Arabidopsis* antibacterial defense. *Proceedings of the National Academy of Sciences, USA* 110: 2389–2394.
- Zhai J, Jeong DH, De Paoli E, Park S, Rosen BD, Li Y, Gonzalez AJ, Yan Z, Kitto SL, Grusak MA *et al.* 2011. MicroRNAs as master regulators of the plant NB-LRR defense gene family via the production of phased, trans-acting siRNAs. *Genes & Development* 25: 2540–2553.
- Zhang X, Zhao H, Gao S, Wang WC, Katiyar-Agarwal S, Huang HD, Raikhel N, Jin H. 2011. *Arabidopsis* Argonaute 2 regulates innate immunity via miRNA393(*)-mediated silencing of a Golgi-localized SNARE gene, *MEMB12*. *Molecular Cell* 42: 356–366.
- Zvereva AS, Pooggin MM. 2012. Silencing and innate immunity in plant defense against viral and non-viral pathogens. *Viruses* 4: 2578–2597.

Supporting Information

Additional Supporting Information may be found online in the Supporting Information section at the end of the article.

Fig. S1 Effect of RNA silencing on *BIR1* expression in plants infected with TuMV.

Fig. S2 Epigenetic regulation of *BIR1* and RdDM-methylation controls.

Fig. S3 Methylation status of the *BIR1* promoter using whole-genome bisulfite sequencing (WGBS) data in *Arabidopsis*.

Fig. S4 Methylation status of the *BIR1* promoter using in-house bisulfite sequencing in *Arabidopsis*.

Fig. S5 Epigenetic regulation of *BIR1* and RdDM-methylation controls in salicylic acid (SA)-treated plants.

Fig. S6 *BIR1* mRNA accumulation in RNA silencing mutants, cleavage mapping at the 5' UTR of *BIR1* mRNA and viral accumulation in *N. benthamiana* leaves expressing *BIR1*.

Fig. S7 DEX-inducible system for overexpression of *BIR1* in *Arabidopsis* plants.

Fig. S8 Phenotypes of *BIR1*-overexpressing transgenic *Arabidopsis*.

Fig. S9 Phenotypes of *BIR1*-overexpressing transgenic seedlings grown in axenic conditions.

Fig. S10 Model of *BIR1* regulation.

Table S1 List of primers.

Please note: Wiley Blackwell are not responsible for the content or functionality of any Supporting Information supplied by the authors. Any queries (other than missing material) should be directed to the *New Phytologist* Central Office.